

# **Closed-die forging and slab hot rolling with focus on material yield**

**Some industrial problems  
analysed by FEM**

**ESA ERVASTI**



**KTH Industrial Engineering  
and Management**

**Doctoral Thesis in Production Engineering  
Stockholm, Sweden 2008**



**KTH Industrial Engineering  
and Management**

# **Closed-die forging and slab hot rolling with focus on material yield**

**Some industrial problems  
analysed by FEM**

**Esa Ervasti**

Doctoral thesis in Production Engineering  
Stockholm, Sweden 2008

TRITA-IIP-08-01  
ISSN 1650-1888  
ISBN 978-91-7178-871-9

KTH School of Industrial Engineering  
and Management  
Department of Production Engineering  
Royal Institute of Technology  
SE-100 44 Stockholm, Sweden

Academic thesis, which with the approval of Kungliga Tekniska Högskolan, will be presented for public review in fulfilment of the requirements for a Doctorate of Engineering in Production Engineering. The public review is held at Kungliga Tekniska Högskolan, M311, Brinellvägen 68, at 10.00 on the 25:th of April 2008.

© Esa Ervasti, April 2008

## Abstract

The thesis is focussed on improving the material yield in closed-die forging and rolling. The former is restricted to the manufacturing of heavy crown wheels and front axle beams and the latter to the hot rolling of steel slabs. To enhance the yield the commercial FE-codes Form2D and Dyna3D are used. Results from forging simulations are strengthened by full scale experiments. The research is carried out in near contact with the Swedish steel and engineering industry. In closed die forging, two bulk forming problems are treated: How to improve the tool design and how to change the pre-form geometry for decreasing the amount of material exiting the flash gap? In slab rolling, two problems related to material defects are considered: How to eliminate existing surface cracks and how to prevent the formation of voids around macro-inclusions embedded in the steel matrix? Internal voids might be the reason for scrapping the whole workpiece.

Considering the forging of crown wheels, a new concept is proposed. For making the central hole of the product, the traditional method was forging a thin circular plate which was then sheared off and scrapped. Using the new technique this operation is replaced by forging a conical tap in the centre, which is then discarded. Doing so, the inner scrap material decreased with about 15%. The idea has been used in production for seven years. – Regarding the forging of front axle beams, a quasi-3D method is used comprising full scale measurements of the axial material flow. Here the theoretical material yield increased 2-7%.

Regarding rolling, the initial surface cracks in the simulations are V-shaped with a crack angle of  $6^\circ$  and of depth 5-20 mm. The inclusions are cylindrical and either three times harder or three times softer than the matrix. The behaviour of the cracks and the inclusions are studied as influenced by process parameters. Current industrial input data are used as a reference. – It is concluded that longitudinal cracks cannot be totally eliminated. During rolling their V-shape gradually changes to Y-shape and a remaining oxide flake separates the crack bottom surfaces. For minimizing the detrimental influence of the entrapped oxide, an early closure of the crack bottom is important. Throughout the remaining rolling schedule the entrapped oxide is then torn to pieces with large areas of virgin metal in between ensuring a strong bond. The following recommendations are given for the longitudinal cracks: Light drafts/pass at the beginning of the rolling schedule followed by heavy ones. – Contradictory to longitudinal cracks it is concluded that transversal cracks are possible to eliminate. When eliminated, the initial bottom of the crack coincides with the slab surface. No folds are formed. For the transversal cracks light drafts/pass are proposed together with reversal rolling, the latter for avoiding crack folding. – Voids are easiest formed around hard macro-inclusions in the centre of the slab. Large rolls and heavy drafts are recommended to avoid this.

Keywords: Material yield; Closed-die forging; Hot rolling; Cracks; Macro-inclusions; Steel; FEM.

## Acknowledgements

First of all I would like to thank my supervisor Professor Ulf Ståhlberg for his fruitful support and patience. Together with him valuable ideas were hatched in a warm environment. I have not only got knowledge but also a good friend in him.

I want to thank all my colleges at the research group of Materials Forming, Department of Production Engineering, Royal Institute of Technology, for a great time and stimulating discussions.

Great thanks are put forward to L. Henningson, H. Karlsson, B. Bohlström and D. Axelsson for making it possible for me to carry out full-scale counter blow hammer forging experiments at JOT-components Wirsbo AB. I also want to thank M. Bylund, J. Ångman and A. Nilsson for great help with forging experiments performed in the big eccentric press at Imatra Kilsta AB. Considering experiments referred to rolling I put forward my gratitude to Harry Pettersson, SSAB Tunnplåt AB, for valuable ideas and access to reference process data. Thanks are also put forward to my DYNA-support, Ragnar Nilsson.

Finally I would like to give my appreciation to my wife Rita for her encouragement, backing and tolerance during this work and to my parents Irma & Väinö for their backing and confidence through all my years of studies. Without their support the finishing writing of this thesis had never been done. Thanks also to my children Daniel, Antonia and Gabriel for making me bring this work to the end.

Stockholm, 2008-01-20

Esa Ervasti

## Dissertation

The thesis is built on a summary and the following papers:

- Paper A     E. Ervasti and U. Ståhlberg, A new closed-die forging concept for the manufacturing of crown wheels in: *Advanced Technology of Plasticity*, Proceedings of the 6<sup>th</sup> ICTP, Vol. 111, 1999, pp 1663-1668.
- Paper B     E. Ervasti and U. Ståhlberg, A quasi-3D method used for increasing the material yield in closed-die forging of a front axle beam, *Journal of Materials Processing Technology* 160 (2005) 119-122.
- Paper C     E. Ervasti and U. Ståhlberg, Behaviour of longitudinal surface cracks in the hot rolling of steel slabs, *Journal of Materials Processing Technology*, 94 (1999) 141-150.
- Paper D     E. Ervasti and U. Ståhlberg, Transversal cracks and their behaviour in the hot rolling of steel slabs, *Journal of Materials Processing Technology*, 101 (2000) 312-321.
- Paper E     E. Ervasti and U. Ståhlberg, Void initiation close to a macro-inclusion during single pass reductions in the hot rolling of steel slabs, *Journal of Materials Processing Technology*, 170 (2005) 142-150.

## Contents

1.	Introduction .....	1
2.	Material yield in closed-die forging and slab hot rolling .....	4
2.1	Closed-die forging .....	4
2.2	Hot rolling .....	6
3.	Summary of papers .....	7
3.1.	Paper A: “A new closed-die forging concept for the manufacturing of crown wheels” .....	10
3.2	Paper B: “A quasi-3D method used for increasing the material yield in closed-die forging of a front axle beam” .....	17
3.3	Paper C: “Behaviour of longitudinal surface cracks in the hot rolling of steel slabs” .....	21
3.4	Paper D: “Transversal cracks and their behaviour in the hot rolling of steel slabs” .....	27
3.5	Paper E: “Void initiation close to a macro-inclusion during single pass reductions in the hot rolling of steel slabs” .....	32
4.	Concluding remarks .....	38
5.	References .....	39
6.	Papers: A, B, C, D and E	

# 1. Introduction

For companies, making their profit on metal forming processes such as forging and rolling, a high material yield has become increasingly important. An essential reason is the escalating prices of the raw materials caused by the earth's shrinking mineral resources. Extensive recycling of metals and alloys has become necessary. In metal forming processes the amount of scrapped material must be decreased. Efficient use of the material includes a long life time of the product in service. Consequently the products must be of accurate geometry and free from outer and inner imperfections. However the raw material includes different types of defects such as cracks, voids, heavy segregations and inclusions. For eliminating them or for making them less harmful, it is of great importance that adequate process parameters are used during the plastic deformation.

Considering closed-die forging much effort has been put to decreasing the amount of flash. This is especially true for heavy components of complex shapes such as crankshafts and beams. When new tools are designed for increasing the material yield, the shapes of the pre-form and the dies – pre-forging die and finishing-forging die – must be well adapted to each other. Further more, the die design must ensure that there is no risk for the creation of folds. In recent times precision forging processes, flashless or near net shape forging, have been established in the automobile industry for small axis-symmetric parts, e.g. gearwheels and steering pinions. This way of reducing the material waste, contributes to the ongoing cost-saving trend in the automobile industry, [1]. Further development of this technology to bigger and more complex parts, e.g. connecting rods, is expected to lead to a wider implementation in industry. – In the hot rolling of slabs automatic gage and width control is used to reach adequate final dimensions also for slab regions neighbouring the long and short sides of the workpiece.

The thesis is focussed on improving the material yield in closed-die forging of components and in hot rolling of steel slabs. The simulations are concentrated on the material flow and they are all carried with industrial data as a reference. In forging focus is put on reducing the scrap material by improving the die design or the shape of a roller reduced pre-form. In rolling the yield is heavily dependent on the quality of the as-cast slab. Frequently surface cracks and inner macro inclusions are present. Here some possibilities to minimise their detrimental influence, by choosing optimal process parameters, are presented. The thesis is divided into two parts focussing the material yield from two aspects; tool design and raw material quality. The relations between the different papers of the thesis are presented in (Fig. 1).

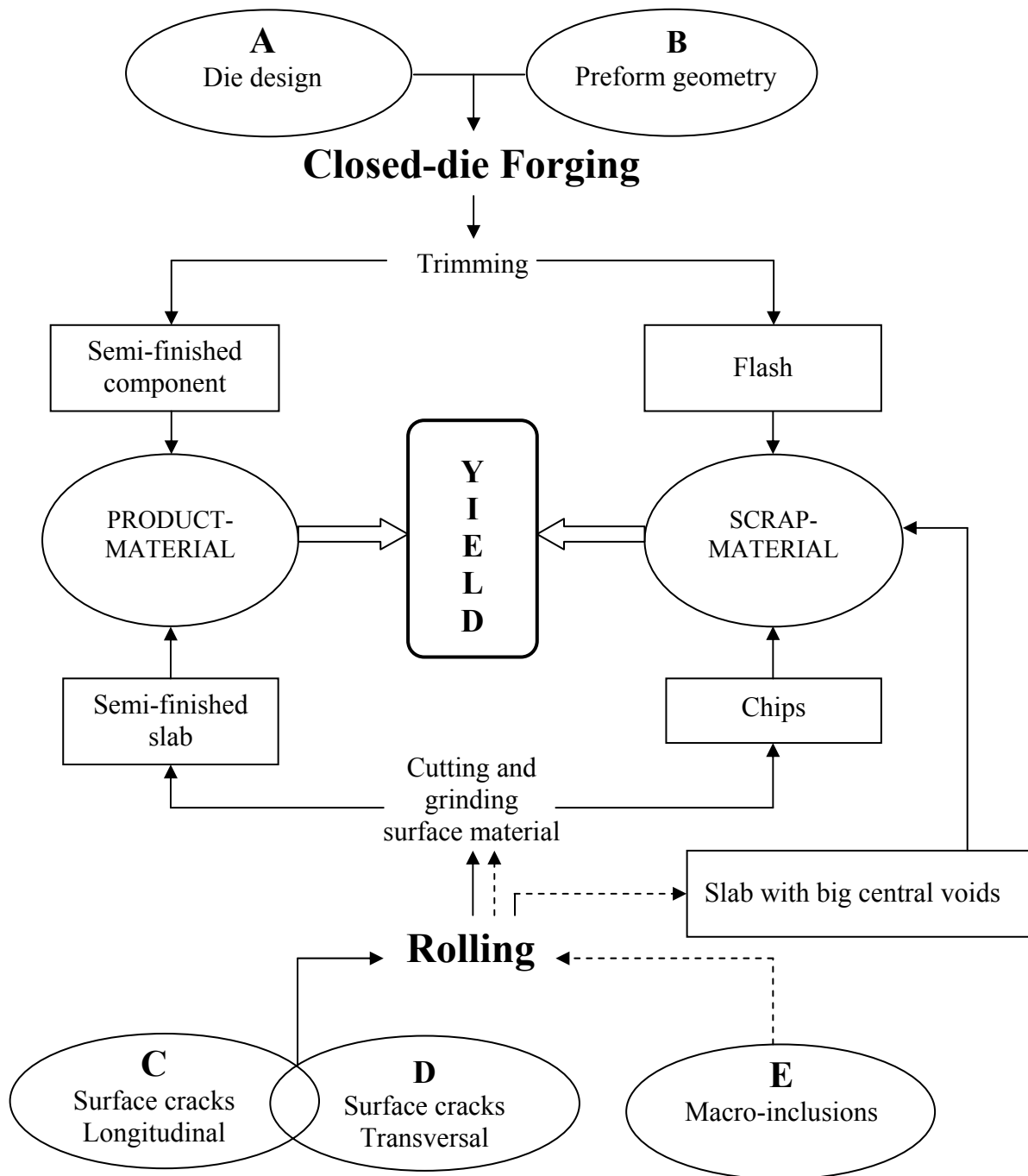


Fig. 1. Relationship between the papers of the thesis.

## 2. Material yield in closed-die forging and slab hot rolling

In many hot working processes the value added by means of the forming itself is small. This fact gives the material yield a high economical priority. The material losses in the hot working of steel may have many reasons. Some are related to geometry such as fish tails and overlaps in slab rolling and flash and folds in closed-die forging. Such imperfections are discarded. Sometimes whole products are classed down because they are totally out of shape or furnished with big cracks or inclusions and voids. For removing oxides and surface cracks and to obtain the accurate dimensions of the product some kind of machining is generally necessary. Hot working processes are always associated with oxidation. According to Samolyk and Pater [2], closed-die forging processes are characterized by a material waste amounting on average to about 20% of the forging mass. The total material loss in Europe in the 1990s has been estimated to 360 000 tonnes per year.

### 2.1 *Closed-die forging*

#### 2.1.1 Cavity filling

If the die cavities are not completely filled the product is out of dimensions and therefore scrapped. An analytical expression describing conditions for cavity filling is presented by Tomov et al., [3]. This work is focussed on flash land dimensioning. Another work treating this subject is presented by Samolyk and Pater [2] who use the slip-line field method for flash-land design. Their analysis is compared with forging simulations performed with the finite element method. Also these authors study cavity filling as influenced by the flash land geometry, however they also incorporate the forging load. Keife and Ståhlberg [4] present numerically optimized plane-strain upper-bound solutions for various flash designs meant for the forging of a spindle. The metal flow just before and after cavity filling is analysed. Theory is compared with plasticine experiments. It is concluded that a flash land comprising a V-notch puts an effective brake on the material when it flows towards the flash gap. However the load is heavily increased.

In *Paper A*, a new type of die design is proposed for the forging of a heavy crown wheel. Earlier forging of a central plate in the middle of the workpiece is replaced by forming a conical tap, which after the finishing blow is sheared off and scrapped. When designing the conical part of the die, the main objective was to save material. Within the optimising procedure, FE-simulations were carried out for a lot of bottom cone radii and draft angles combinations. In this paper three conditions of different character were used for the design. They are related to early cavity filling, a maximum load and a maximum energy.

In *Paper B* only one of these conditions, early cavity filling, is used for increasing the material yield in 2-stage forging of a big front axle beam. The current 2-stage forging was fed by preforms of complex shape from a roller reducing mill. In this work, the possibility to improve the yield by introducing a new pre-form shape built on nothing but circular cross sections along its length is analysed.

### 2.1.2 Adaptation of the preform to the finishing die geometry

If the pre-form and dies in multi-step forging are not well adapted to each other the material yield will be poor and the risk for defect formation high. A numerical method for optimising the shape of pre-form dies in two-stage hot forging is presented by Poursina et al., [5]. The object of optimisation is to prevent workpiece defects that may arise during the forging process. A two dimensional finite element code is developed for predicting imperfections. Sedighi and Tokmechi [6] treat the design of pre-forms meant for complex parts and underline their heavy influence on loads and material wastes. The authors propose a new algorithm for practical design. Results for two various die sets show that the material waste could be reduced by 5.1 - 7.3% at the same time as the forging loads decreased. Park and Hwang [7] analyse the forging of rib-web type aerospace- and aircraft components, which are characterised by small fillet and corner radii with zero draft angles. They point out that an improper pre-form invokes defects of underfilling and folding with excessive stresses and wear of the dies. The researchers present an attempt to design the preform for precision forging of an asymmetric rib-web component. This is done by means of a rigid-plastic finite element analysis.

In *Paper B* the forging of a front axle beam is analysed. The forming starts with a roller reduced pre-form. This workpiece is then pre-forged and finally finished forged. From the finished forged product it became clear that three cross sections along the billet length were associated with a large amount of flash why they were regarded as critical. For improving the yield, it was decided that the forging of these sections should be followed through the manufacturing by means of a quasi-3D analysis built on 2D simulations and experimental estimation of the axial material flow. By furnishing the current pre-form with a series of contiguous marks it was possible to relocate the critical sections from the finished forged product to the workpiece after pre-forging and after roller reducing. This was done in production. For improving the material yield the current pre-form shape should be changed. Contradictory to this pre-form the new one should be built on nothing but circular cross sections along its length. Thus it became possible to carry out the 2D simulations for the three critical sections. Here the experimentally established positions of the sections were used. The 2-step analysis was carried out for circular pre-form areas, which were stepwise decreased. The simulations were stopped when underfilling occurred.

By using measured areas of the old sections, after the different forming steps, it was possible to compensate the 2D results for the axial material flow. Thus the 2D results could be corrected to 3D and used as guidelines for designing the grooves of the roller reducing mill. – This quasi-3D method is rapid and well suited for a first scanning of similar problems (forming of long products). It is believed that such an introductory analysis, followed by just a few time-consuming 3D simulations, could decrease the computer time considerably. The method is similar to that proposed by Ståhlberg in [8]. The only difference is that in [8] an empirical spread formula replaces the area measurements. A detailed description of the quasi-3D approach is given in the summary of *Paper D*.

### 2.1.3 Closing of voids

The closing of metallurgical defects in cross-sections of forgings are reported in several studies. A summary is given by Poursina et al., [5]. In this paper, works by Park and Yang [9], [10] and by Ståhlberg and Keife [11] are mentioned.

The closing of voids is not incorporated in the thesis. However the process parameters recommended in *Paper D* for preventing the evolution of voids around a hard macro-inclusion in slab rolling are in agreement with those recommended for closing of voids in forging.

## 2.2. Hot rolling

### 2.2.1 Closing of central holes

The quasi-3D model [8] mentioned earlier was meant for the closure of a central longitudinal hole in hot rolling between flat and parallel rolls. The behaviour of the defect is modelled by plane strain upper bound solutions of the Johnson type [12] together with the empirical Wusatowski spread formulae [13] and stress states as determined from the slip-line field theory. According to the model, rolling conditions resulting in large spread are favourable.

### 2.2.2 Preventing the formation of voids around inclusions

An excellent two-level model is presented by Luo [14] in which uncoupled macro and micro models are utilized. They are used for simulating the local behaviour of the material close to very small non-metallic inclusions during the hot rolling of steels. The stress history of the sub-volume in the macro-model, including workpiece and rolls but not the inclusion, is employed as boundary loading conditions for the micro-model comprising both inclusion and steel matrix. The approach is described into

detail in [15] together with the influence of process parameters such as rolling temperature, rolling reduction and friction on the roll/workpiece interface. Simulations are carried out for two rolling temperatures, 1200° and 800°C. At the higher temperature a silicate inclusion is ductile and at the lower almost undeformable. At the high temperature the inclusion is softer than the matrix and no voids are formed. Voids are however evolved around the rigid imperfection. Moreover, the risk for void formation is found high for inclusions close to the surface due to strong tensile stresses acting in the horizontal directions.

In *Paper E* macro-inclusions are treated and consequently the need for a mesomechanical approach is small. This is a straight forward paper with focus on the influence of process parameters and on the inclusion locations. The yield stresses of the inclusions are simply set to 3 times bigger and 3 times smaller than the matrix and the most dangerous case of zero friction and cohesion on the inclusion/matrix interface is chosen. When a comparison is possible, the agreement between *Paper E* and papers [14] and [15] is good considering recommendations for a high material yield. In the present paper however, void formation around macro-inclusions located very close to the surface were not investigated.

### 2.2.3 Closing of surface cracks

The behaviour of transversal surface cracks on the slab corner during vertical and horizontal (V-H) rolling with flat vertical roll and grooved vertical rolls is analysed by Hai-liang YU et al. [16]. This was done by the explicit dynamic finite element method. The closure and growth of cracks as influenced by contact pressure from the rolls was analyzed. The calculated results are in good agreement with experiments.

It is difficult to compare this work [16] with *Paper C* and *Paper D* because the authors treat different types of well defined surface cracks. In *Paper C* the behaviour of a central longitudinal crack is simulated and in *Paper D* a transversal one. – According to simulations presented in the thesis the transversal crack, but not the longitudinal, is possible to eliminate by using the correct process parameters and rolling schedules. For improving the material yield by efficient removal of transversal cracks light drafts/pass together with a small roll radius is recommended. Reversal rolling is optional for avoiding folding of the two opposite surfaces of the V-crack. The best results are obtained for low friction. – The recommendations for the longitudinal cracks are similar when the very beginning of the rolling schedule is considered. The reason is that, for light drafts/pass, the V-shaped crack quite rapidly changes to Y-shaped. Doing so, the bottom of the crack is folded with a thin oxide flake in between. From now on it is recommended to change to heavy drafts/pass. Further folding is difficult to get. During the remaining heavy elongation of the slab, the

embedded oxide film will be broken up to very small flakes with large areas of welded virgin metal in between. In this way an almost perfect bond between the bottom side surfaces of the crack is obtained.

### 3. Summary of papers

The simulations are carried out by means of two commercial FE-codes, the implicit Form2D [17] for closed-die forging and the explicit Dyna3D for rolling. The latter is described by Hallquist in [18]. One reason for using Form2D in the forging simulations is that this program incorporates automatic remeshing, which is necessary for fast computations of a non-steady state process. However, Form2D cannot handle rotating tools. This is the reason for using Dyna3D which is well suited for steady state processes such as rolling, at the same time as the time for computation becomes acceptable. In Form2D the tools are treated as rigid bodies and the workpiece as an isotropic visco-plastic material with a flow stress depending on strain, strain-rate and temperature. The mesh is characterized by iso-parametric triangular six-node elements with one node in each corner and one node on each side. It is described by Kobayashi et al. in [19]. A summary of the general formulations is presented in Eqs. (2.1-2.3). Six stress components are needed as well as three velocity components for each node.

$$\int_V \sigma'_{ij} \delta \dot{\epsilon}_{ij} dV + \int_V \sigma_m \delta \dot{\epsilon}_v dV = \int_S F_i \delta v_i dS \quad (2.1)$$

The incompressibility equation can be written as

$$\int_V \delta \sigma_m \dot{\epsilon}_v dV = 0 \quad (2.2)$$

where  $\sigma'_{ij}$  represents the stress field,  $\sigma_m$  the mean stress and  $\delta v_i$  the velocity components.  $V$  is volume,  $S$  surface area,  $\delta \dot{\epsilon}_{ij}$  strain rate,  $\delta \dot{\epsilon}_v$  volumetric strain rate and  $F_i$  the nodal force. The common elemental vectors of unknowns are  $\{v^e\}$  and  $\{\sigma_m^e\}$ . The equation derived from Eqs. (2.1) and (2.2) to be solved is

$$[K]\{v\} = \{f\} \quad (2.3)$$

where  $K$  is stiffness matrix,  $f$  the applied force vector and  $v$  the velocity vector.

The equation is non-linear due to viscosity, which is a function of the flow stress and the effective strain-rate. Form2D uses direct iteration to solve the system. In this way the velocities and the hydrostatic pressure fields are

obtained. The code uses incremental updating of the time steps for obtaining the change in workpiece geometry.

Dyna3D has a high flexibility in modelling the rolling process. The FE-model is based on Eq. (2.4), where  $\sigma_{ij,j}$  is the Cauchy stress tensor,  $\rho$  the current density,  $f_i$  the body force density and  $\ddot{x}_i$  the acceleration, [18].

$$\sigma_{ij,j} + \rho \cdot f_i = \rho \cdot \ddot{x}_i \quad (2.4)$$

Based on process data, the geometries of the slab and rolls are generated. For the slab 8-node hexahedron elements are used. Hourglass force resistance vectors are applied to prevent the formation of hourglass energy according to a paper by Flanagan and Belyotschko, [20]. The rolls are represented by rigid shell elements. No roll flattening is permitted. The mesh of the workpiece is generated together with the defect – a surface crack or an inclusion. The geometry of the defect is based on recommendations from the industry.

Once the mesh has been generated, boundary forces are applied on loaded surfaces. The work roll is loaded with a momentum to generate the necessary rotational velocity. Nodal constraints are limitations in degrees of freedom used to keep the work roll fixed in a stable position during each pass with a specified angular velocity. At the start of rolling one short side is loaded in the rolling direction to generate the movement of the strip into the roll gap. The load used is removed from the surface as soon as gripping has been observed for not violating the simulation results. The force has been given a value high enough for accelerating the workpiece into the roll gap. However this force must not result in a compression stress exceeding one 10th of the flow stress.

Schwer et al., [21] describe how Dyna3D selects the minimum value of time step  $\Delta t_1, \Delta t_2, \dots, \Delta t_N$ . over all elements, Eqs. (2.5, 2.6) where  $a$  is a recommended scale factor set to 0.15 for obtaining stability.

$$\Delta t^{i+1} = a \min\{\Delta t_1, \Delta t_2, \Delta t_3, \dots, \Delta t_N\} \quad (2.5)$$

$$\Delta t^{n+1/2} = \frac{\Delta t^n + \Delta t^{n+1}}{2} \quad (2.6)$$

Courant stability is a requirement that must be considered by choosing a penalty factor. Penalty functions are used to prevent nodes from one part to penetrate another one, [21]. The penalty factor shall not exceed a critical value, which violates the stability criterion. According to Felippa [22] a characteristic time step, which is ten times larger then the Courant time step is chosen where  $K_n$  is the elemental stiffness and  $m_n$  is the mass.

$$\Delta t \leq \frac{2}{\omega_{\max}} = \frac{2}{\sqrt{\frac{K_n}{m_n}}} = 2\sqrt{\frac{m_n}{K_n}} \quad (2.7)$$

The summary of paper *Paper A* below is given more space than *Paper B*, *C*, *D* and *E*. The reason is that this conference paper is too short for giving a full description of the strategy used for tool design. The complementing figures found in this summary are found in [23] and [24].

### **3.1 A new closed-die forging concept for the manufacturing of crown wheels**

The aim of the present work is to increase the material yield with 1 kg in the manufacturing of heavy crown wheels of weight 43.7 kg (Fig. 2). The components are made from cylindrical bars of height 287 mm and diameter 160 mm. To begin with, the billet is heated to 1280°C and then upset forged to 60 mm in a mechanical press. After that the workpiece is closed-die forged by a counter blow hammer in nine blows all of 200 kJ. Each hammer head weights 25000 kg and each tool 1500 kg. When the forging starts the velocities of the upper and lower dies are approximately 2.72 m/s. After the finishing blow, the flash and a thin central circular plate (Fig. 3a) of weight 4 kg are sheared off and scrapped. The crown wheel is then furnished with cogs by machining. During the finishing blow only a very small part of the total energy from the hammer is available for plastic deformation. Further forging is not possible. The principle of a counter blow hammer is shown in (Fig. 4), [25].

For improving the material yield a new die design is proposed. For the current concept, the “neutral plane” is found at the very centre of the workpiece. This means high tool pressures with a maximum at the middle of the plate (Fig. 3b) and a big forging load, especially towards the end of the forging sequence. Because of the fact that the hammer is energy bounded, a big force means a small displacement between the tools. This explains the large number of blows. In fact a big part of the plastic energy is used for forging the scrap material. During the last blow the workpiece height decreases only 0.05 mm compared with 28.9 mm during the first. The corresponding values for the energies used for plastic deformation are 1.5 % and 84 % respectively, of that delivered by the hammer. Consequently a large amount of the supplied energy is transferred to the forging machine and not to the workpiece, when the finishing blow is considered.

By introducing a new tool design where the central part of the plate is replaced by a conical tap (Fig. 5a) the “neutral plane” will no more be found in the centre (Fig. 5b). Instead of a maximum contact pressure at the centre of a plate, a minimum of zero is found at the free top surface of a cone. This means that the forging can be done by smaller loads. Consequently the plastic energy delivered by the hammer will result in larger drafts and thereby in a less number of blows. The geometry of the conical cavity is optimised with respect to load, energy, early die filling and practical aspects. The geometrical parameters analysed are clear from (Fig. 6) where  $\alpha$  is the semi-cone angle,  $R$  the bottom radius of the cone,  $r$  the tap corner radius and  $\beta$  a small angle at the bottom of the tap meant for adjusting the main directions of the material flow.

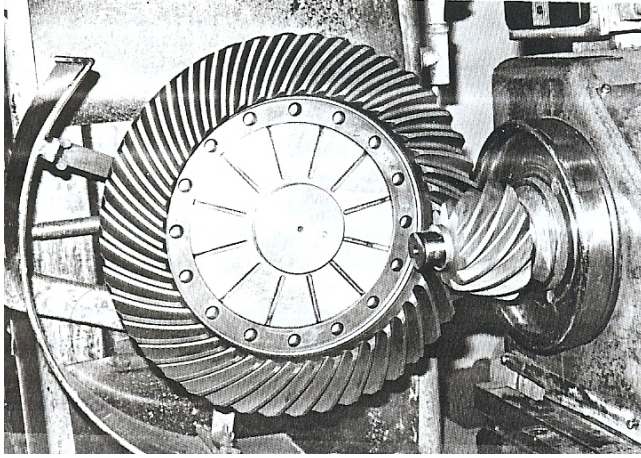


Fig. 2. A crown after machining the cogs, here working together with pinion in a transmission [23].

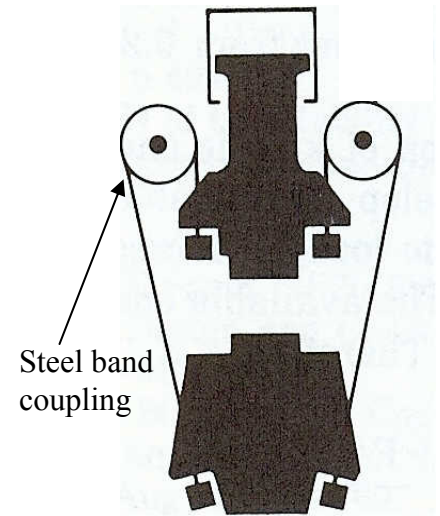


Fig. 4. Principle of a counter blow hammer [25].

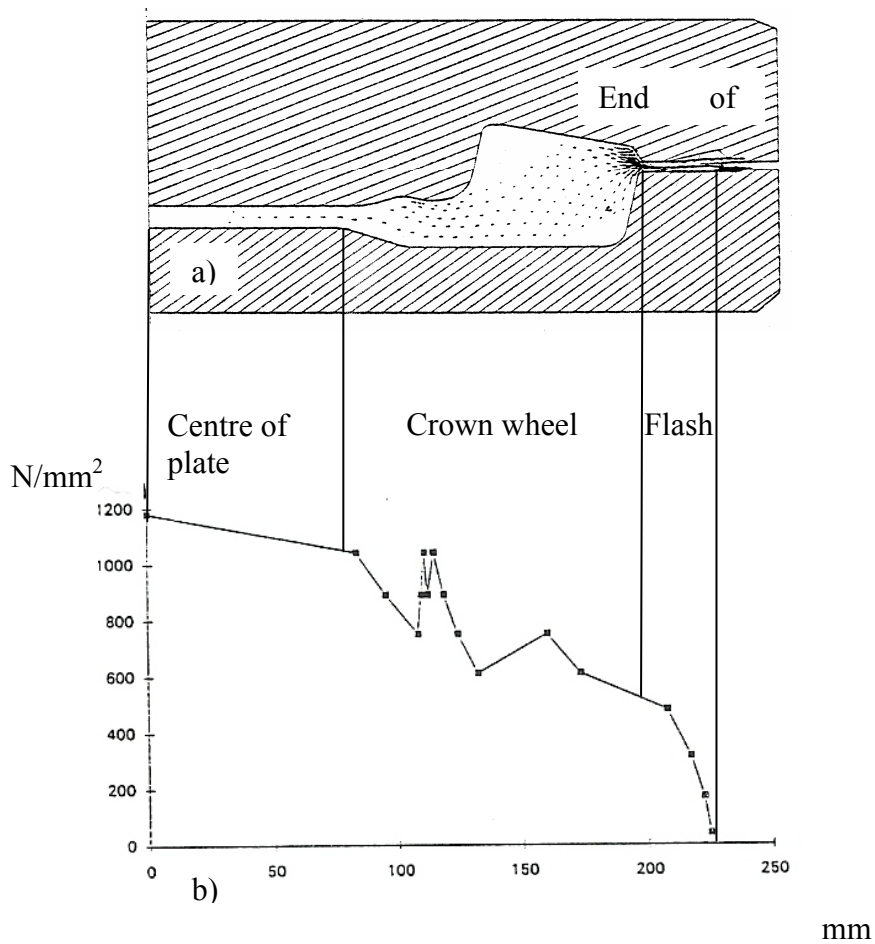


Fig. 3 (a-b). (a) Material flow at the end of the finishing blow when forming a crown wheel and (b) Pressure distribution on the upper die cavity

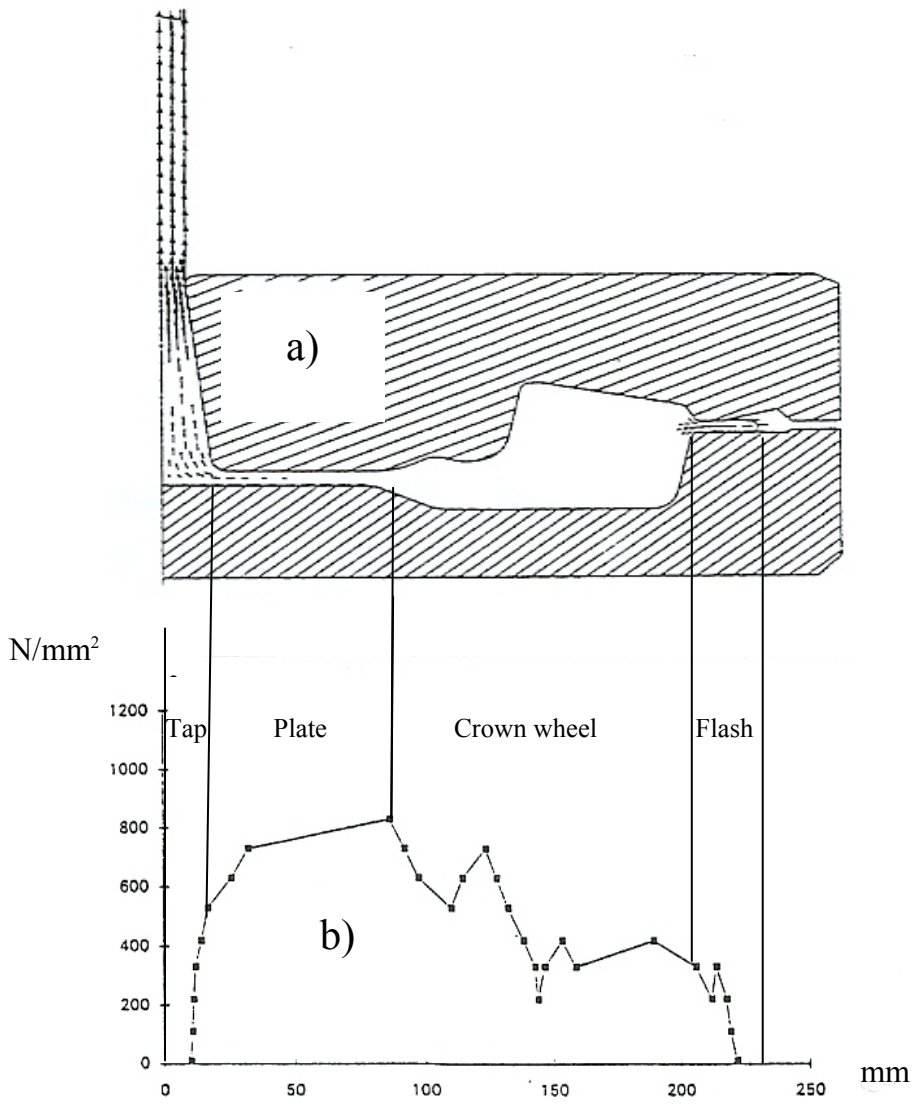


Fig. 5. (a-b) New tool design, single tap, including (a) the material flow during the last blow and (b) the tool pressure distribution showing a maximum close to the outer radius of the thin plate [24].

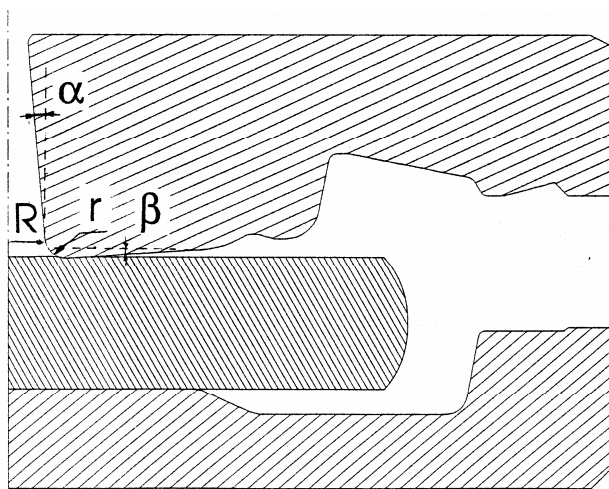


Fig. 6. Geometrical parameters defining the conical part of the die.

The simulations were carried out for a workpiece weight decreased by 1 kg. The current bar used in production was cut shorter in length. Thus a successful series of forging simulations should indicate that the goal set up was reached. The magnitudes of all nine drafts were chosen the same as for the current forging. These were determined by stop tests and sample measurements. The upper and lower tool velocities were supposed to decrease linearly from 2.72 m/s to zero. In order to take the tool retardation into account, which was not possible with Form2D, all nine drafts  $d$  were divided into 5 equal increments  $\Delta d_i$  and their corresponding mean values of  $v_i$  within each increment were used. For establishing the friction coefficient, simulations were compared with an experiment. The diameter of the contact surface between the workpiece and the lower crown wheel cavity was measured in production after the 1<sup>st</sup> blow. Simulations with different friction coefficients were then carried out. Equal diameters in experiment and simulation determined its value to 0.12.

The simulations meant for design of the new die then started. To begin with the influence of  $\alpha$  and  $R$  was investigated for  $r=10$  mm and  $\beta=0^\circ$  (Fig. 6). The simulation scheme is shown in Table 1a. The semi cone angle  $\alpha=0^\circ$  is just used as a reference. The load  $F$  required during the last blow is considered of special interest because if this force is low, the final dimensions of the product can be obtained by means of this energy bounded machine. The sum of plastic energies  $W$  used in the nine blows is of interest for the number of blows necessary for forming the product. The reason for marking some simulation results grey in Table 1a is that one or more of the following criterions are not fulfilled:

1. The maximum load  $F$ , which is found during the ninth draft must be smaller for the new concept. If satisfied, the ratio between the new and old load is presented on white background.
2. The sum of plastic energies  $W$ , needed for the nine drafts (blows) in production,  $d_1, d_2, \dots, d_9$ , must be smaller for the new concept. If satisfied, the ratio between the new and old sum of energies is presented on white background.
3. The “crown wheel cavity” must be filled latest during the ninth blow. If so, the letter  $C$  on white background appears in the Table.
4. The conical part of the cavity must also get filled. If so the letter  $T$  appears on white background in the Table.

According to these criterions there are several combinations of parameters that could be accepted. In Table 1b geometries that don't satisfy all conditions 1-4 have been taken away. The final simulation result – the best one – is presented on white background in Table 1c. According to the criterions the lowest force  $F$  in the final blow made the choice,  $\alpha=5^\circ$  and  $R=15$  mm. Further simulations showed that  $\beta=3^\circ$  instead of  $\beta=0^\circ$  improved the results (Fig. 6).

However, the blue window shows the industrial choice which is commented below.

Table 1(a-c)

(a) Data used in the forging simulations together with results, (b) Geometries fulfilling the conditions 1-4, (c) Final result from simulations, showing the lowest load in the last blow; white background. Practical aspects determined the final tap geometry for production; blue background.

R (mm)	$\alpha$							
	0° (reference)		5°		10°		15°	
10	W>	C	0.9484	C	W>	C	W>	C
	F>	T	0.9573	T	F>	T	F>	T
15	0.8484	C	0.9612	C	W>	C	W>	C
	0.9829	T	0.9420	T	F>	T	F>	T
20	0.7498	C	0.8351	C	0.9646	C	0.9028	C
	0.7009	T	0.9829	T	0.9689	T	F>	T
25	-	-	0.8204	C	0.8466	C	0.9032	C
	-	-	0.7875	T	0.8955	T	0.9573	T

a)

R (mm)	$\alpha$			
	0°	5°		15°
10		0.9484	C	
		0.9573	T	
15		0.9612	C	
		0.9420	T	
20		0.8351	C	0.9646
		0.9829	T	0.9689
25				

b)

R (mm)	$\alpha$			
	0°	5°		15°
10				
15		0.9612	C	
		0.9420	T	
20			0.9646	C
			0.9689	T
25				

c)

As said by industry, the new forging concept resulted in a tap height which was too big. In practical forging the workpiece – including the tap – must be totally enclosed in the die. If the result obtained from the simulations were used (Fig. 5a) the upper tool should become too big and heavy, and therefore difficult to handle. Further more, if an upper die of the same thickness as the current one should be employed, the load should increase drastically when the tap gets in contact with the roof of the cavity. For decreasing the tap height, new simulations were carried out, this time for a conical cavity with  $\alpha = 5^\circ$ ,  $R = 15$  mm *also* in the lower die (*double tap*). This solved the problem. In Fig. 7, the material flow is shown for the last blow. The tap height is considerably lower for the “double tap concept” and both taps are totally enclosed by the tools.

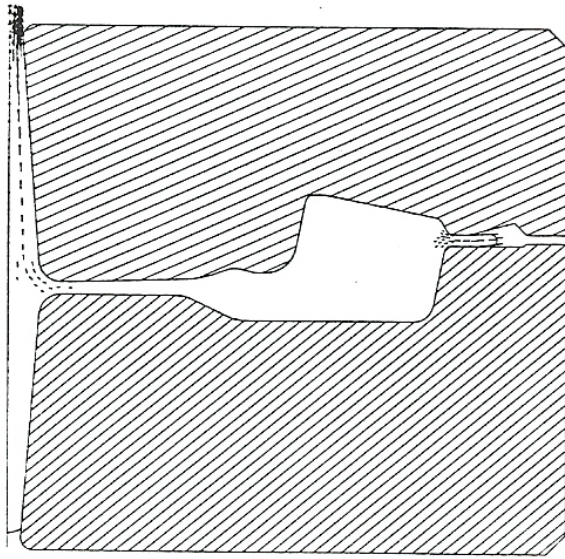


Fig. 7. New tool design with a double tap. The material flow is included for the final blow [24].

This design was however not accepted either. More practical aspects must be considered. The forged specimen must be easy to remove from the die cavity. Thus the industrial choice presented in the blue window (Table 1c) was  $\alpha = 10^\circ$ ,  $R = 20$  mm,  $\beta = 3^\circ$  and  $r = 10$  mm. This geometry is found in Table 1b among geometries fulfilling the four listed criteria. In order to save tool material and to ensure early cavity filling, the bottom tap was made lower than in (Fig. 7).

The load during the 9<sup>th</sup> blow was found a little bit higher than that accepted by the 4 conditions. However, it had become clear that the total plastic energy needed for the new concept was much lower than for the old. Consequently it was supposed that the number of blows could be decreased and thereby a less drop in workpiece temperature was expected. This means a softer material and a smaller load in the practical finishing forging.

Full scale experiments were carried out with the new tools. They showed that the number of blows was reduced from 9 to 6 and that the objective to increase the material yield with 1kg was reached. The new concept was used in production during the years 1996-2003. The productivity was improved by 30-40%. Earlier 1000 crown wheels could be forged before the tool had to be taken out of production. The new design managed to manufacture 1500 crown wheels. On the basis of the 6 drafts, the material flow at the end of blow no 2, 3 and 4 are presented in (Fig. 8). The old and new concept are compared in (Fig. 9) showing the stepwise deformation during the blows needed.

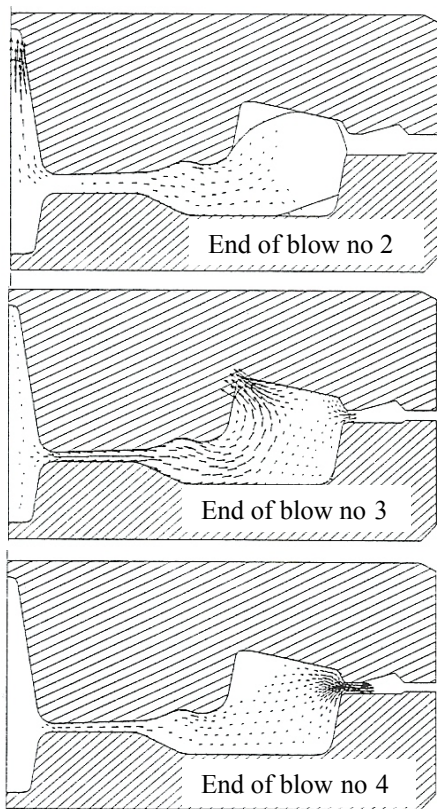


Fig. 8. Final die design. Material flow at the end of blows no 2, 3 and 4. Only six blows are needed for forming the product.

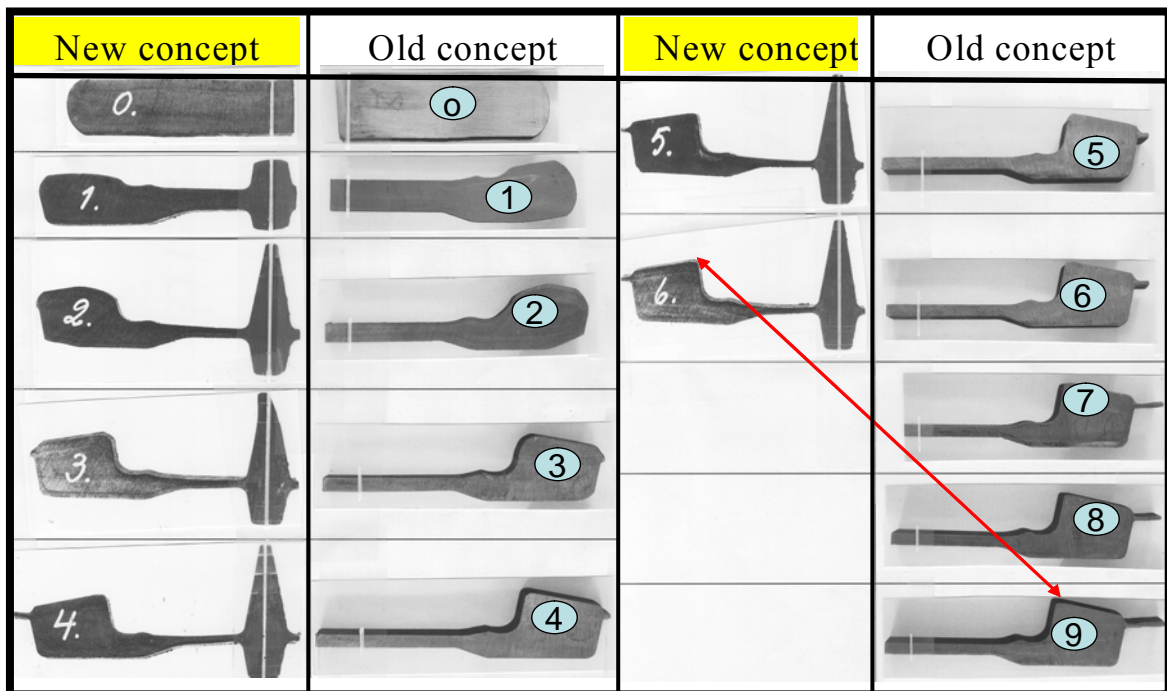


Fig. 9. A comparison between the new and the old concept. The material yield is improved at the same time as the number of blows is decreased.

In *Paper A* the practicable benefits of the results are treated more into details.

### 3.2. A quasi-3D method for increasing the material yield in closed-die forging of a front axle beam

The material yield in the forging of a front axle beam was poor. The weight of the billet was 115.4 kg and approximately 30% was recycled as scrap. The current preforms – obtained from a roller reducing mill – were built on square and round cross-sections. It was decided that the possibility to improve the yield by exchanging the current pre-form with one built on nothing but circular geometries must be investigated. If satisfying results were obtained, the roll pass design must be changed. The forming was performed as 2-step closed-die forging. Cavity filling without defects is the only criterion used when designing the tools.

The aim of the work was to find the optimum shape of the new pre-form so that the material yield could be improved. It was decided that the new forming of the front axle beam should be analysed by 2D-simulations and that the results should be compensated with the axial material flow found for the current production. To begin with three cross sections marked C-C, D-D and E-E on the finished forged beam were classified as critical considering the material yield in the current production (Fig. 1). The forming of them should be simulated for a new pre-form built on circular cross sections. Thus the position of the three cross sections had to be identified after roller reducing and after roller reducing + pre-forging. After that the cross sectional areas after every deformation step was measured for establishing their stepwise change in area in the 2-step forging that was caused by the axial material flow. The nine cross-sections are presented in (Fig. 2). In the simulations, those obtained directly from the roller reducer mill were transformed to circular pre-form shapes and constituted the first pre-form in a series of 2D simulations where the pre-form area was decreased stepwise until underfilling occurred in the 2-step forging. These optimal pre-form sections were then compensated for the material flow in the axial direction. A more detailed description of the quasi-3D method is given below. For easing the description, the following notations are introduced.

$A_0^{prod}$	Measured pre-form cross-sectional area of square or round shape after roller reducing
$A_1^{prod}$	Measured pre-forged cross-sectional area
$A_2^{prod}$	Measured finished-forged cross-sectional area
$A_0^{2D}$	$A_0^{prod}$ transferred to circular shape for 2D simulations.
$A_0^{2D_{min}}$	Minimum cross-sectional area of circular shape for filling the 2D cavities
$A_0^{3D_{min}}$	Minimum cross-sectional area of circular shape for filling the 3D cavities

#### Subscript

$i$	Cross sections C-C, D-D and E-E
-----	---------------------------------

1. The three cross-sections  $(A_0)_i^{prod}$  (Fig. 2) are measured.
2. The areas are transformed to circular shapes,  $(A_0^{2D})_i$  and used in the of 2D-simulations for improving the material yield.
3. The material flow for sections  $(A_0^{2D})_i \rightarrow (A_1^{2D})_i$  and from  $(A_1^{2D})_i \rightarrow (A_2^{2D})_i$  are studied during pre-forging and finishing forging. Cavities which have been filled without problems enter the 4<sup>th</sup> step for forging a smaller initial area  $(A_0^{2D})_i$ .
4. A series of simulations is started.  $(A_0^{2D})_i$  is decreased stepwise until underfilling occurred in one of the two dies. Then the simulations were interrupted. The areas used in the second last 2-step simulations are denoted  $(A_0^{2D}_{min})_i$ . They constitute the results from the 2D-simulations.
5.  $(A_0^{2D}_{min})_i$  is then transformed to  $(A_0^{3D}_{min})_i$  by compensating for the maximum loss in area caused by material flow in axial direction. This compensation is based on the full scale experiments in the current production.

$$(A_0^{3D}_{min})_i = (A_0^{2D}_{min})_i + (\Delta A^{max})_i \quad (1)$$

$$(\Delta A^{max})_i = [(A_0)_i^{prod} - (A_1)_i^{prod} ; (A_0)_i^{prod} - (A_2)_i^{prod}]_{max} \quad (2)$$

If  $(\Delta A^{max})_i < 0$  then  $(\Delta A^{max})_i$  is set to zero.

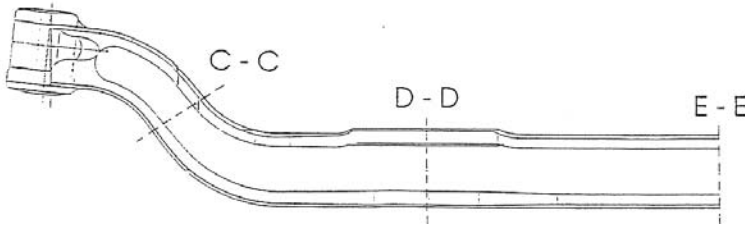


Fig. 1. “Critical” sections marked C-C, D-D and E-E [24].

An eccentric press of capacity 16 000 tons was used for the forging. The principle of such a machine is presented in (Fig. 3). The front axle beam after pre-forging and finishing forging is shown in (Fig. 4).

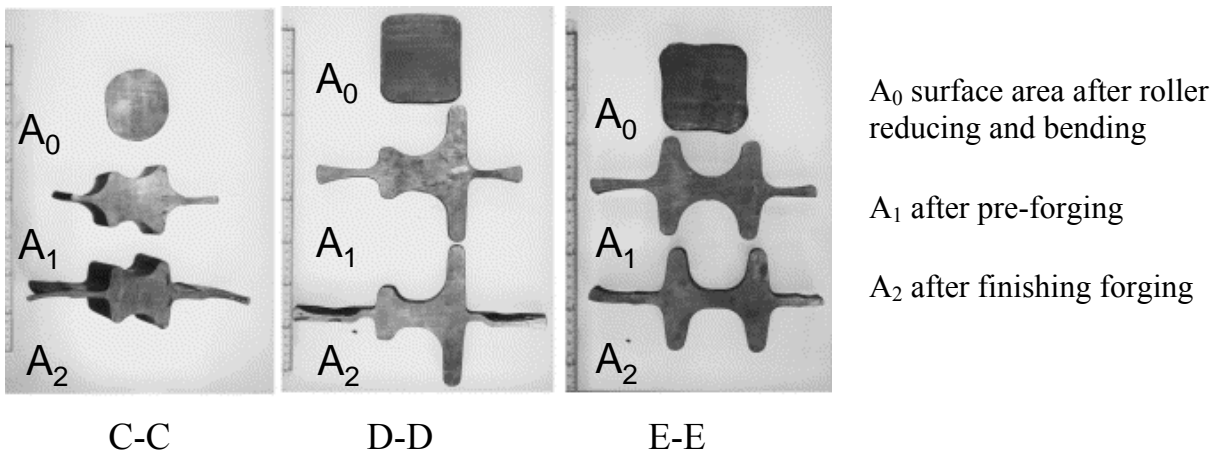


Fig. 2. The nine cross-sections analysed in the manufacturing of the front axle beam.

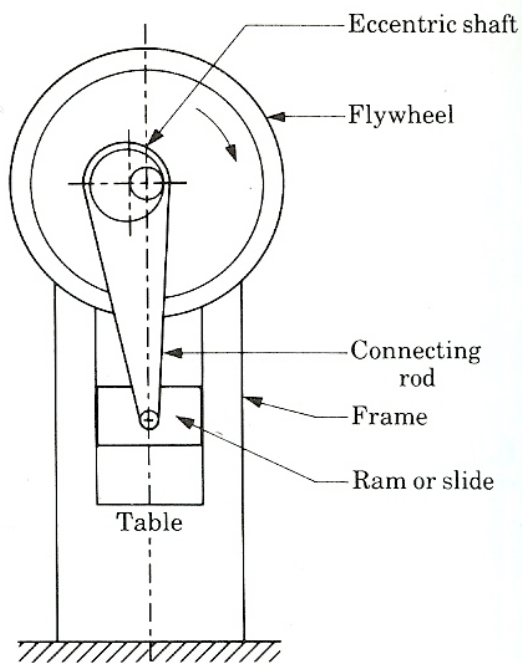


Fig. 3. Schematic picture showing the principle of an eccentric press [26].

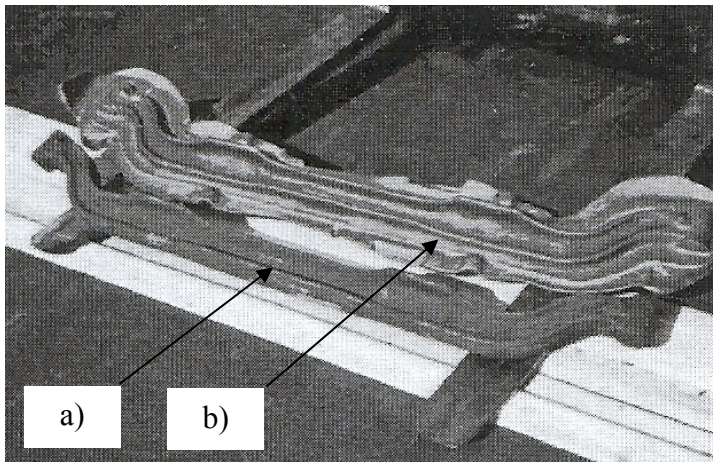


Fig. 4 . Front axle beam after (a) pre-forging and (b) finishing forging including 30% flash material. Billet weight; 115 kg.

The commercial software Form2D [17] was used for the simulations. Some examples showing the material flow in the D-D plane after improvement of the material yield are presented in (Fig. 5). The result from the work is summarised in Table 1.

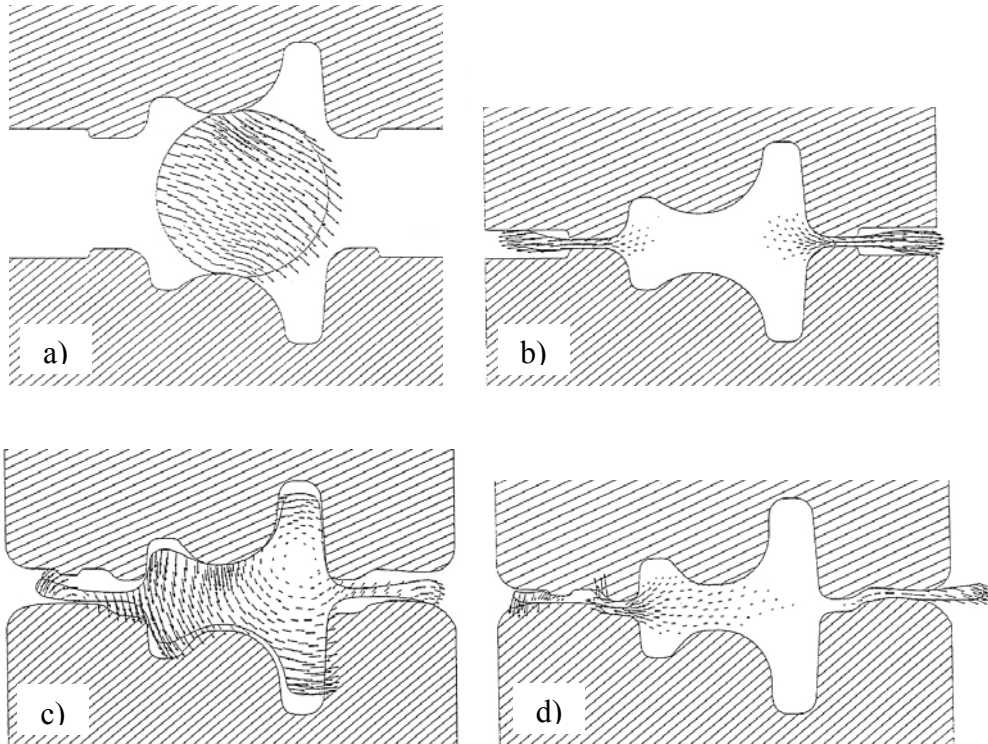


Fig. 5. (a-d) Material flow in section D-D (a) at the beginning of the pre-forging (b) at the end of pre-forging (c) at the beginning of finishing forging and (d) at the end of finishing forging [24].

Table 1  
Results from the quasi 3D-analysis [mm<sup>2</sup>]

Section	$A_0^{\text{exp}}$	$A_1^{\text{exp}}$	$A_2^{\text{exp}}$	$A_0^{2\text{D}}_{\text{min}}$	$\Delta A^{3\text{D}}_{\text{added}}$	$A_0^{3\text{D}}_{\text{result}}$	Improvement
C-C	6426	7159	6822	6138	0	6138	4.5%
D-D	9724	9670	9298	8560	426	8986	7.6%
E-E	6015	6168	5776	5621	239	5860	2.6%

It is found likely that the material yield should increase if the current roll pass design is changed so that the roller reducing mill delivers a pre-form which is built on circular cross-sections. According to the quasi 3D-analysis the material yield for the cross-sections C-C, D-D and E-E can be improved by 4.5%, 7.6% and 2.6% respectively. In production the new pre-form shape was changed to circular cross sections.

### 3.3. Behaviour of longitudinal surface cracks in the hot rolling of steel slabs

In order to improve the material yield by finding the best rolling conditions for minimizing the detrimental effect of longitudinal surface cracks, the influence of process parameters is analysed. It is found that these kinds of cracks are very difficult to eliminate. However it is possible to make them less harmful during the manufacturing. The commercial FE-code Dyna3D is used. The rolls are modelled by shell elements for a rigid material and the slab by brick elements (Fig. 1a.). The crack is modelled V-shaped and of initial depth and angle 20 mm and  $6^\circ$ . The model makes it possible to separate the crack into an upper and lower part (Fig.1b) because they are defined by the angles  $\alpha'$  and  $\alpha''$  respectively. Slabs with cracks deeper than  $h=20$  mm are usually recycled as scrap. A common crack shape is shown in (Fig. 2).

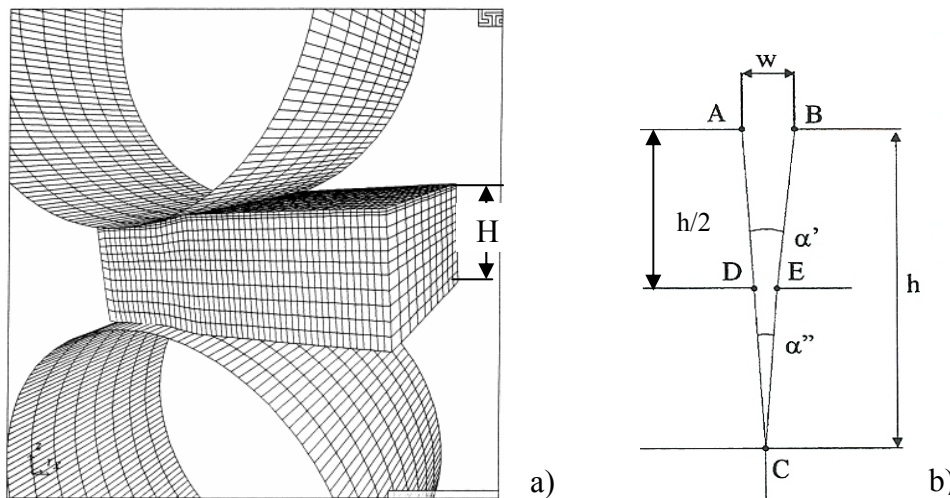


Fig.1. Model used to simulate (a) the roll and work material and (b) the behaviour of a central longitudinal crack.

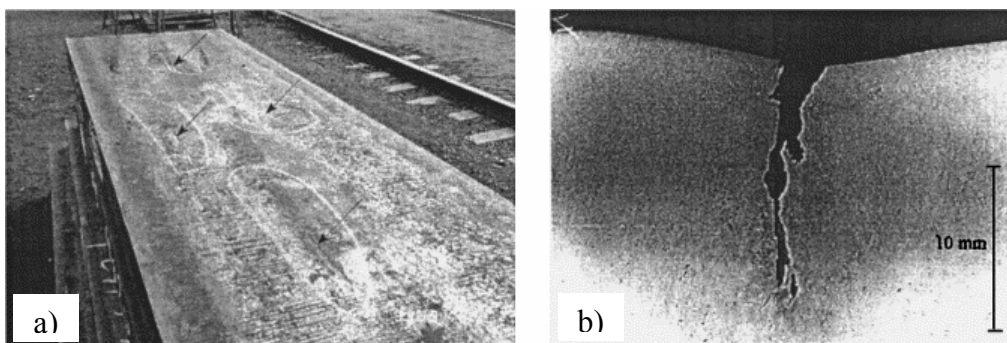


Fig. 2. Long and deep, longitudinal surface cracks; (a) a slab of width and weight 1000 mm and 10 tonnes respectively with cracks located on the surface which are marked by black arrows; (b) a crack deeper than 10 mm.

The influence of rolling schedules is studied for a roll radius 425 mm. An industrial rolling schedule, Series 2 (Fig. 3), is used as a reference for two other schedules, one built on light drafts and the other on heavy ones. The picture shows that the cracks are not eliminated. However, their bottoms are folded,  $\alpha'' = 0$ . At the beginning of the schedule, the crack depth  $h$  follows the thickness reduction of the slab (Fig. 4). The slab thickness is denoted  $H$ . At the end of rolling, the crack depth is reduced less than the slab thickness, especially for heavy drafts.

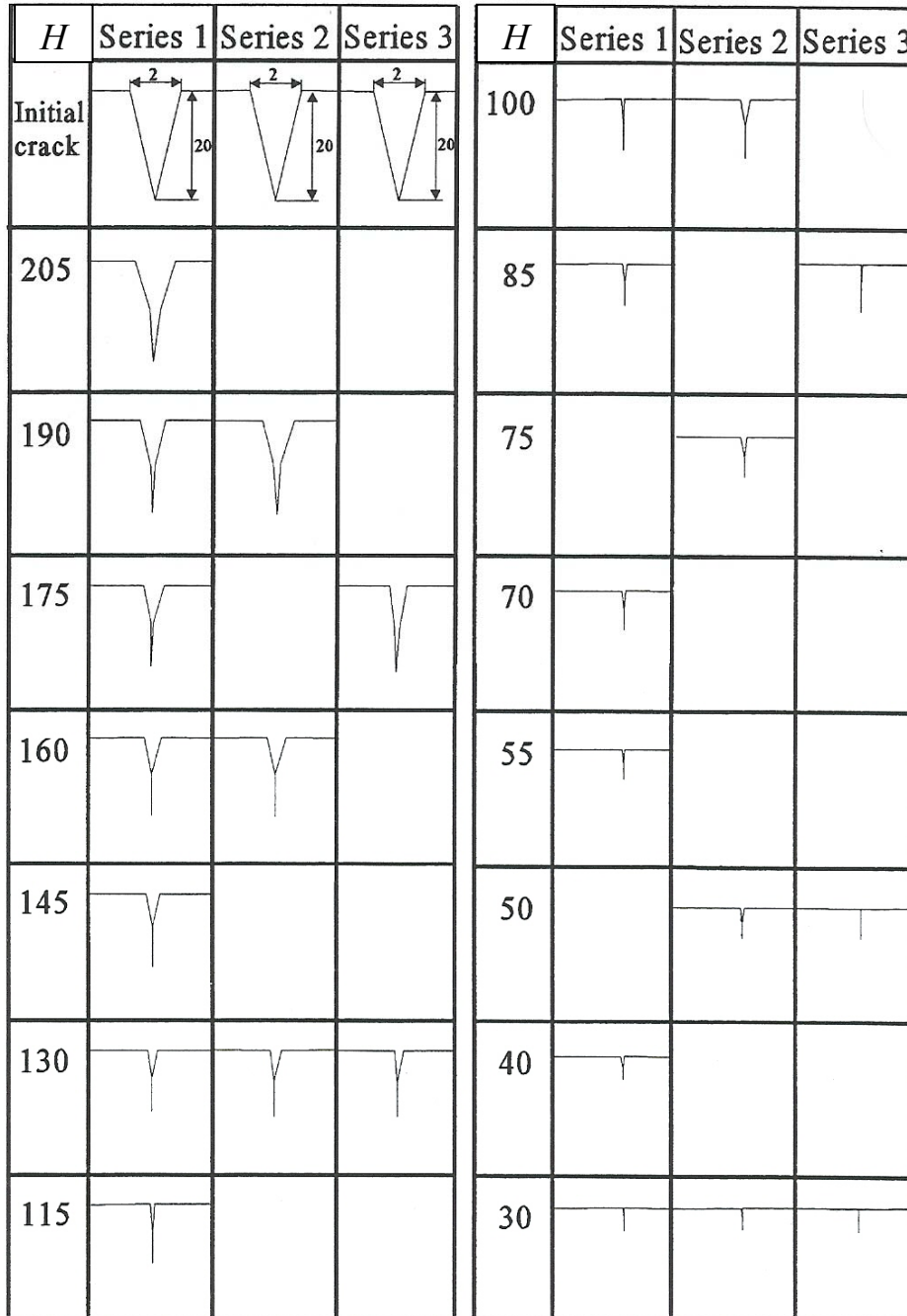


Fig. 3. Surface crack geometries for three rolling schedules covering the deformation from an initial slab thickness 220 mm down to 30 mm.

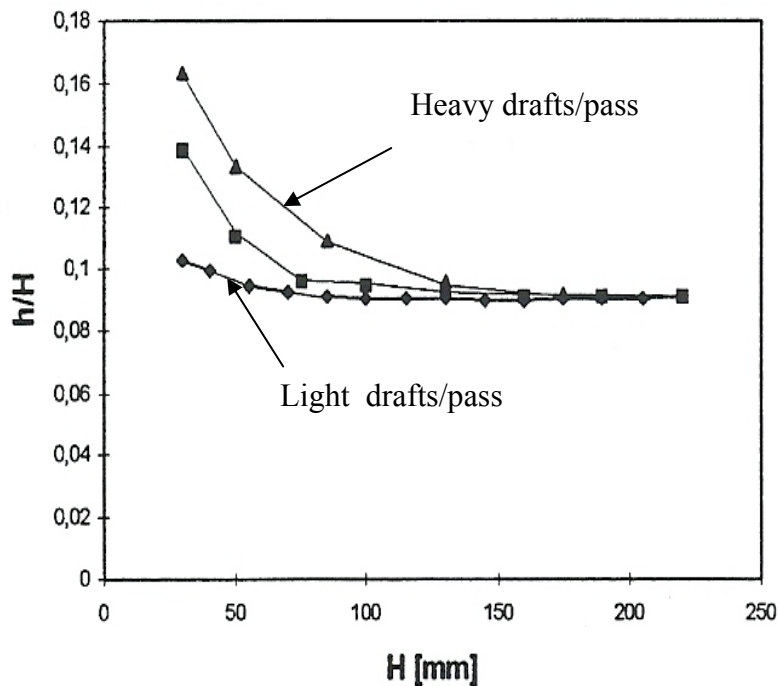


Fig.4. At the beginning of the three rolling schedules, the crack depth follows the reduction that of the slab thickness (horizontal part of the curves). Later however, the crack depth reduction becomes smaller compared to that of the slab, especially for the series built on heavy reductions.

The change in crack width ( $w$ ) for the three schedules is presented in (Fig. 5). It is obvious that the crack is totally closed when heavy drafts are used. This means that the side surfaces of the crack are folded with an oxide flake in between. Then the crack can no longer be up to oxidation.

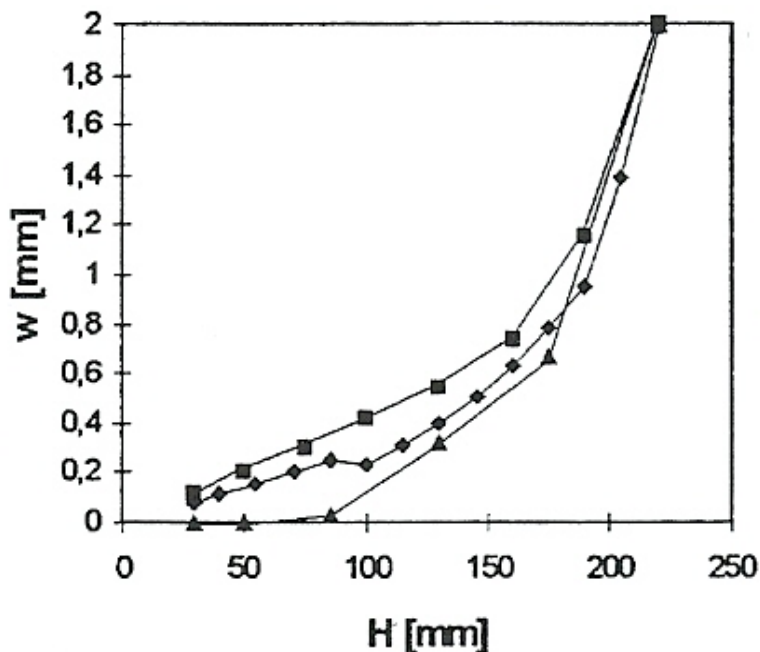


Fig. 5. After three heavy drafts, the slab thickness is reduced from 220 mm to 85 mm and the crack is closed with an oxide film embedded between the side surfaces of the crack.

The deformation of the crack is described more into details with the help of the top and bottom crack angles  $\alpha'$  and  $\alpha''$  (Fig. 6). Light drafts close its bottom part already after 4 passes ( $\alpha'' = 0$ ) corresponding to a decrease in slab thickness from 220 mm to 160 mm. However, the upper part described by  $\alpha'$  is never closed for light drafts. For closing this part of the crack heavy drafts are needed. Then the upper part is closed at  $H = 85$  mm.

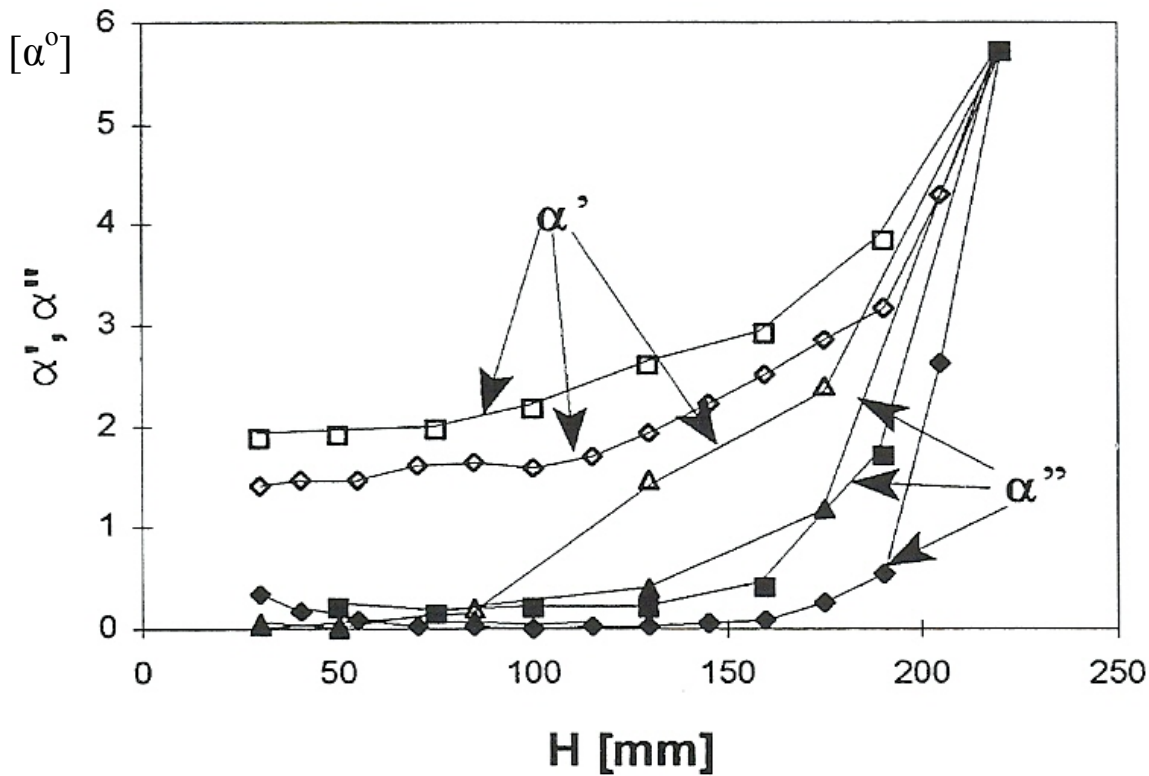


Fig. 6. Change in crack geometry for three rolling schedules. Light drafts close the bottom part of the crack after a slab thickness decrease from 220 mm to 160 mm. However, this schedule does never close the upper part. For heavy drafts both the bottom and the upper part of the crack are closed at a slab thickness of 85 mm.

The accuracy of the simulations was checked for well defined conditions. Thus an experiment in laboratory was carried out with soft aluminium as the model material for the steel. At 400 °C the aluminium showed similar hardening behaviour as the steel at hot working temperature. The rolling experiment was performed for geometrical conditions which are in agreement with the reference mill. Good agreement between experiments and simulations were found (Fig. 7).

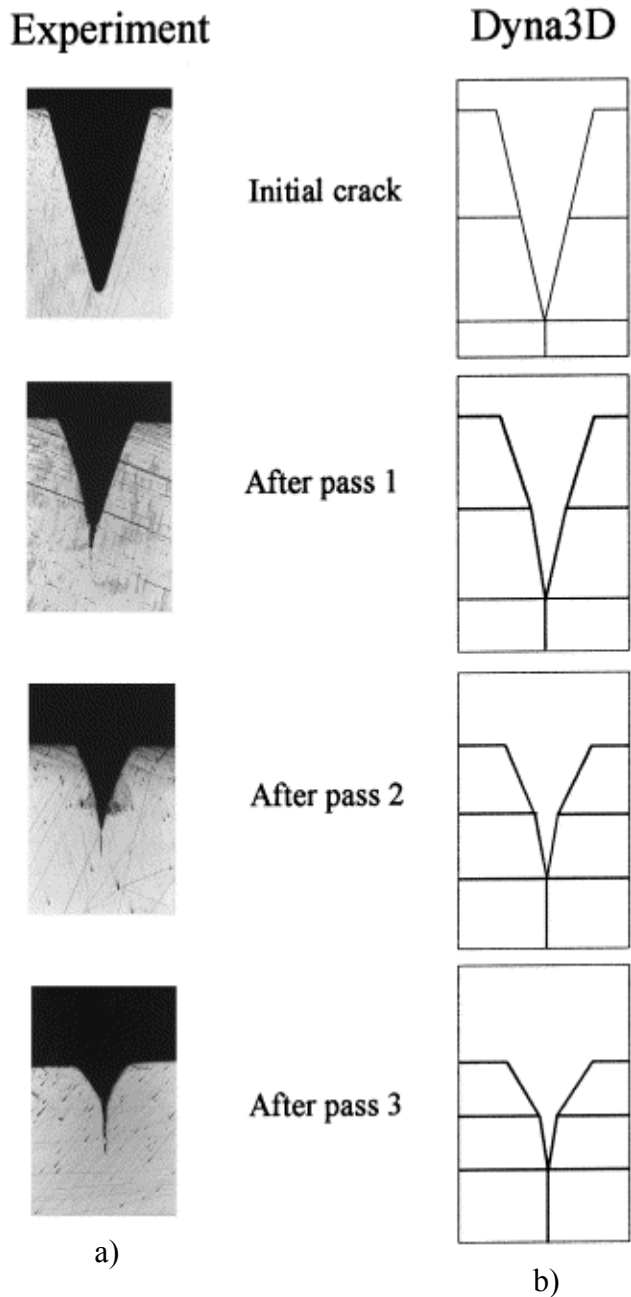


Fig. 7. A comparison between laboratory experiments – with aluminium as the model material for steel – and computer simulations (a) laboratory results (b) simulation results.

To sum up: It is possible to close a longitudinal V-shaped crack by folding its opposite side surfaces. However a more or less serious defect will hang about because of the crack oxidation prior to folding. In fact, even if the crack is totally closed after finishing rolling, a trace of subsurface oxide flakes will remain as an imperfection.

It is clear from the analysis that for heavy drafts/pass, the top and bottom parts of the crack are closed simultaneously, but not until a slab thickness of 85 mm is reached. Then a long and large extended crack area has been oxidised. The possibility to split up the embedded oxide film in an effective way during

the remaining last pass is not considered to be the very best. Consequently it seems reasonable to make use of the fact that for light drafts/pass the bottom part of the crack is closed already at a slab thickness of 160 mm. It seems motivated to recommend light reductions at the beginning of the rolling schedule for closing the crack bottom and heavy ones at the end for closing the upper part. Doing so, further oxidation of the crack bottom will be prevented at an early stage of the rolling. And, because of the remaining heavy elongation of the slab, the deepest oxide film will be efficiently broken up into microscopic oxide particles with a large amount of welded virgin metal in between. It is likely to suppose that shallow imperfections caused by the upper part of the crack only need a light grinding to be removed with an acceptable material yield as a result.

In *Paper C* also the influence of roll radius and friction is treated.

### 3.4. Transversal cracks and their behaviour in the hot rolling of steel slabs

Transversal cracks are analysed in the same principle way as the central longitudinal in *Paper C*. The aim, strategy and boundary conditions are similar so that a comparison between the works is possible. The simulations are carried out for the same industrial mill with a roll radius of 425 mm (as a reference) and an initial slab thickness of 220 mm. The FE-code Dyna3D is used also here. The crack angle is still  $6^\circ$ , however the crack depth is 10 mm instead of 20 mm. Transversal cracks are usually shallower than the longitudinal. Considering this type of crack it has to be pointed out that the rolling is reversal and that this fact influences the results heavily.

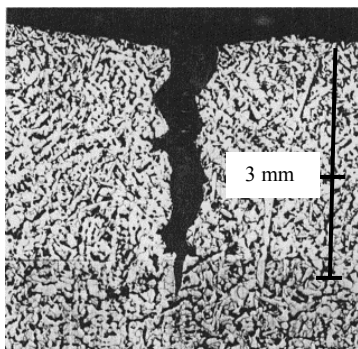


Fig. 1. Transversal cracks are usually shallower than longitudinal. The crack presented was found in an oscillation mark from the continuous casting. The depth of the crack is only 3 mm.

To begin with the behaviour of a transversal crack during its first pass is studied (Fig. 1a). The draft is 30 mm. At the very entrance, the crack widens (Fig. 1b) and within the roll gap it shrinks (Fig. 1c) and finally it opens again (Fig. 1d). At the entrance (Fig. 1a) the peripheral velocity of the roll is higher than that of the slab. Thus the left side of the crack (Fig. 1b) is influenced by a shear stress, which drags it towards the gap while its right side is untouched. This explains the widening. Within the gap (Fig. 1c) the crack is influenced by a high hydrostatic pressure emanating from the roll contact surface. Thus the decrease in width is given a reason for. Finally at the exit, the roll velocity is lower than that of the slab. In (Fig. 1d) the left side of the crack has lost its contact with the roll surface and is no more influenced by it, while the right side is retarded by a shear stress. This explains the second widening.

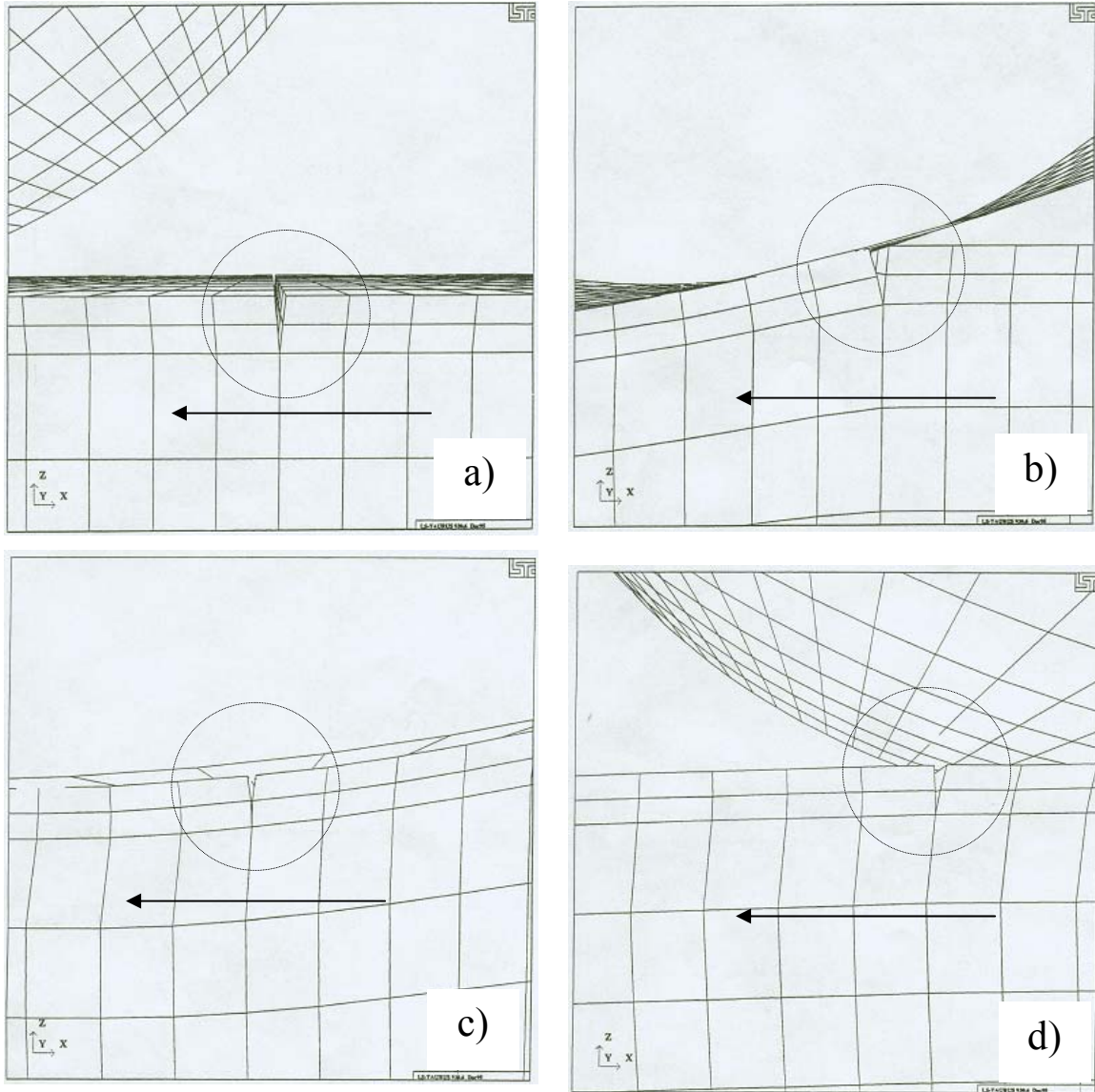


Fig. 2. Crack behaviour during the first pass through the roll gap according to the reference schedule. The draft is 30 mm. The figure shows the crack shape a) before entering the gap, b) at the entrance, c) within the gap and d) at the exit.

Similar to *Paper C*, the influence of three rolling schedules is presented. If the rolling direction was not changed between each pass, it is likely that the opposite sides of the crack should be folded (Fig. 3) resulting in a serious defect. After a rapid glimpse on the series of pictures it seems possible – contradictory to the longitudinal ones – to eliminate transversal cracks without any risk for oxide entrapment. It is obvious that for this kind of crack, a rolling schedule built on light drafts is favourable. At the beginning of the schedules the crack depth ( $h$ ) follows the reduction of the slab thickness ( $H$ ). If small drafts are used (Fig. 4) the crack is up to a heavier height reduction than the slab at the end of the series, at the same time as it widens (Fig. 5). At the end of the series the crack is almost flattened out (Fig. 3), ( $H=40$  mm).

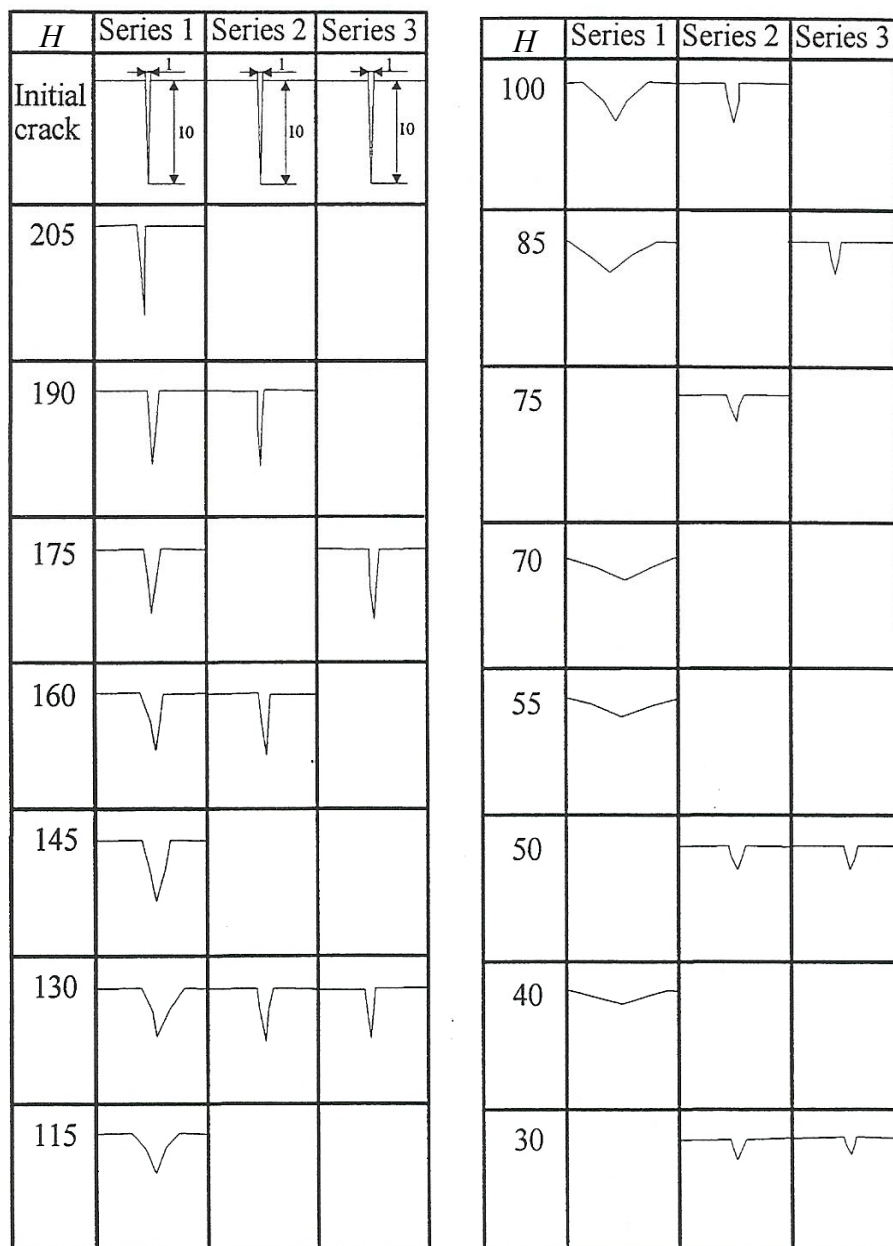


Fig. 3. Surface crack geometries for three rolling schedules from an initial slab thickness 220 mm down to 40 or 30 mm.

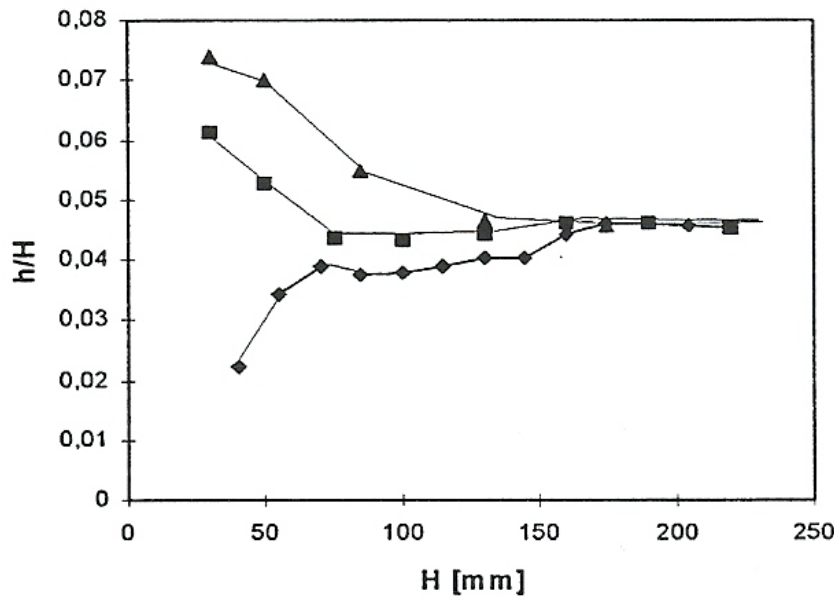


Fig. 4. At the beginning of the three rolling schedules the reduction in crack depth approximately follows that of the slab thickness. At the end of them however, small drafts result in a more rapid crack height decrease.

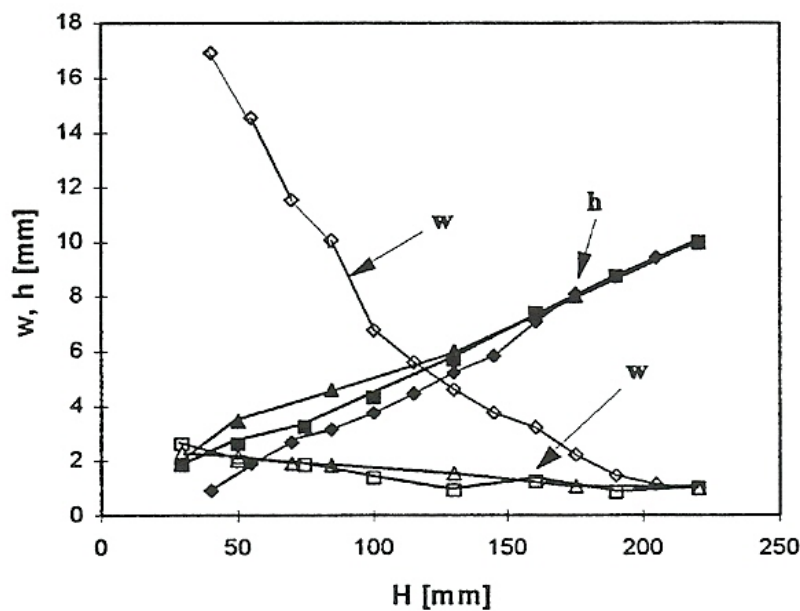


Fig. 5. For light drafts the crack width widens heavily for each passage through the roll gap at the same time as the crack height decreases more rapidly than for heavy drafts.

The change in crack geometry is described more into details by its top and bottom crack angles  $\alpha'$  and  $\alpha''$  (Fig. 6). It becomes clear that both the top and bottom angles increase rapidly for a rolling schedule built on light drafts. Both angles have reached values near  $180^\circ$  after the finishing pass.

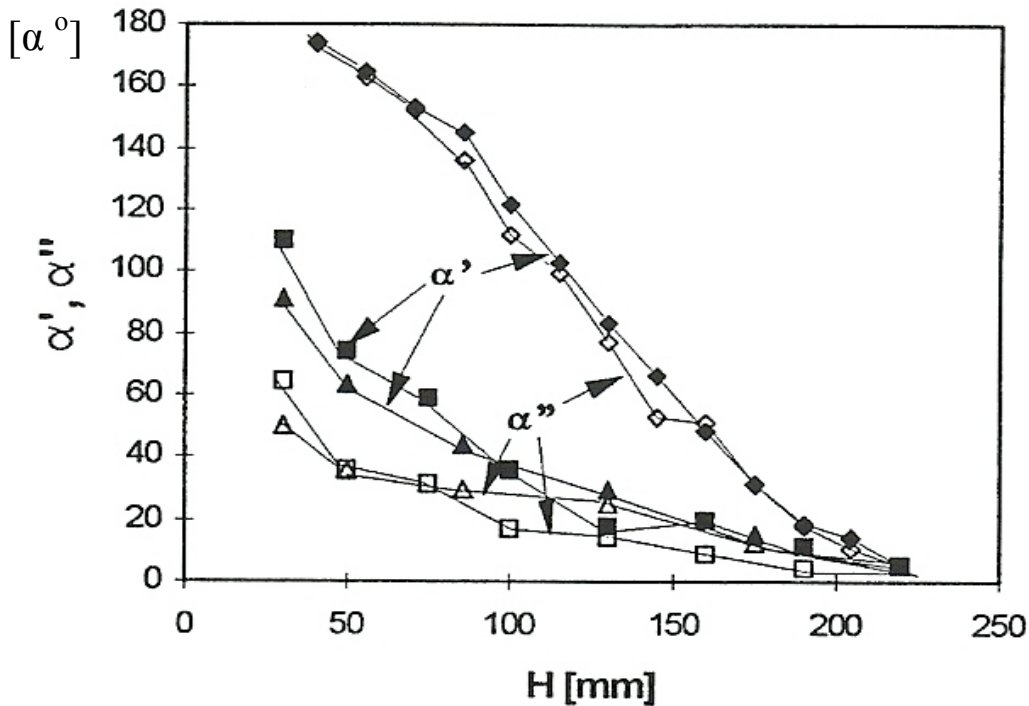


Fig. 6. For light drafts the crack widens rapidly for each passage through the roll gap. This means that the crack is disappearing. Both the top and bottom crack angles are close to  $180^\circ$  at the end of the schedule.

To sum up: For the three schedules presented, the widening is slower for the bottom angle. However it is obvious that transversal cracks compared to longitudinal render less harm. No problems with oxide flakes embedded in folded cracks. And finally, the most important conclusion; it seems possible to eliminate transversal cracks without any grinding. It might be added that full use of this knowledge cannot be implemented because of the resulting low rate of production.

*Paper D* also treats the influence of roll radius, friction and initial crack depth.

### 3.5. Void initiation close to a macro-inclusion during single pass reductions in the hot rolling of steel slabs

Inclusions represent an inescapable type of defect in steels. Non metallic inclusions in steels can be classified into two basic types, those which deform during hot working (i.e. sulfides, silicates) and those which are largely undeformable (i.e. alumina, spinels). Some types of inclusions (i.e. glassy silicates) show a drastic change in viscosity at the non-plastic/plastic transition temperature [27]. Such information is significant when the inclusion behaviour and its affect on the surrounding matrix shall be controlled by choosing adequate rolling parameters such as work temperature. Inclusions may well cause scrapping of the whole slab if the rolling is not performed in an adequate way. For example, voids might be formed around the inclusions which drastically deteriorate the product in service. If big and hard inclusions are found in the steel, the risk for void formation is considerable (Fig. 1a). Soft inclusions are stretched out in the rolling direction (Fig. 1b) and thus flat laminations of varying size and shape are found in the strip.

The aim of this work is to analyse the influence of process parameters on inclusion deformation and void formation. The work is limited to macro inclusions and one pass in slab rolling. Two types of inclusions are studied, one three times harder than the matrix and the other three times softer. In the present work neither cohesion forces nor shear stresses act on the inclusion/matrix contact surface. This is supposed to facilitate the formation of voids. Thus a worst scenario is supposed to be studied. The inclusion treated has a radius of 4 mm and is found in a slab of thickness 220 mm. Software and basic input data are the same as in *Papers C and D*.

The inclusions are cylindrical with an extension through the entire width of the slab. Their size is about 10-100 times bigger than critical micro inclusions. Because it is so big, no mesomechanical approach was needed. The analysis is carried out for different reductions and positions of the inclusions. The locations were chosen to  $H/8$ ,  $H/4$  and  $3H/8$ , measured from the slab surface.  $H$  is the thickness of the slab.

The stepwise transportation of the hard inclusion together with its surrounding steel matrix through the roll gap is presented in (Fig. 2). The inclusion is positioned at  $H/4$  (Fig. 2a). The notation  $L$  that appears in the figures stands for the contact length and  $x=0$  points out the roll gap entrance. The inclusion shows no deformation in (Fig. 2b). However it is twisted clockwise. Two voids appear in (Fig. 2c). Also the voids are twisted and in the same direction. After that, no more rotation is observed. A similar series of pictures is shown in (Fig. 3) for the soft inclusion.

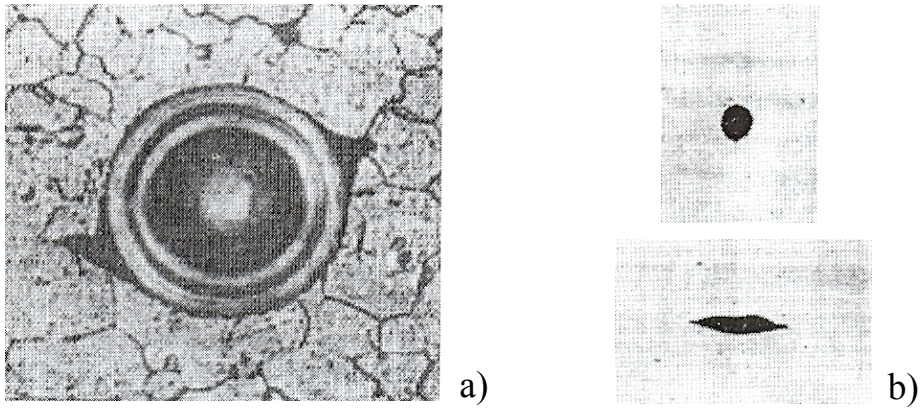


Fig. 1. Slab defects (a) void formation around a hard inclusion and (b) flattening of a soft inclusion.

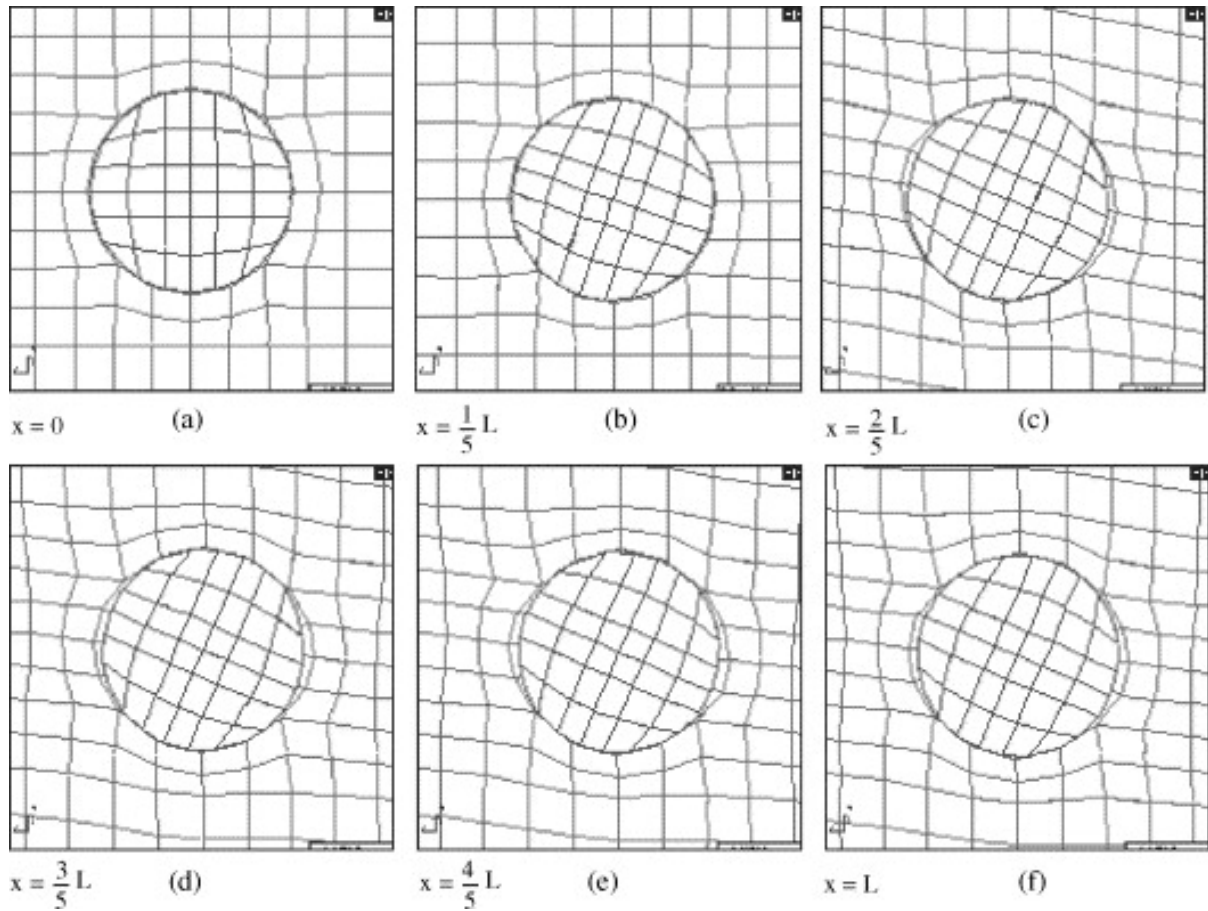


Fig. 2. (a-f) A hard inclusion, positioned at  $H_0/4$ , and its surrounding matrix are traced through the roll gap. Initial slab thickness  $H_0=220$  mm, final slab thickness  $H_1=190$  mm and the initial inclusion radius  $c_0=4$  mm.

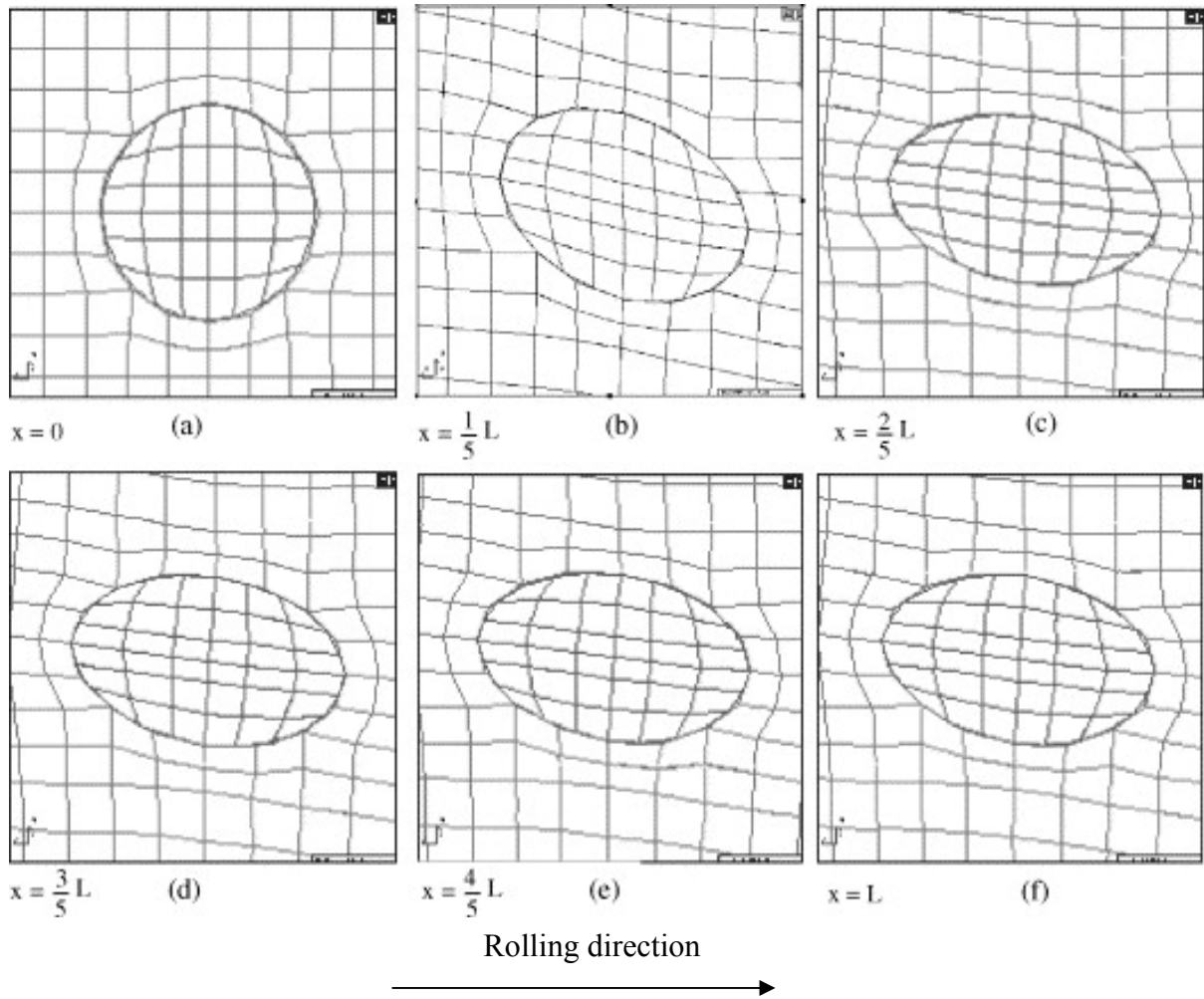


Fig. 3. (a-f) A soft inclusion, positioned at  $H_0/4$ , and its surrounding matrix are traced through the roll gap. Initial slab thickness  $H_0 = 220$  mm, final slab thickness  $H_1 = 190$  mm and the initial inclusion radius  $c_0 = 4$  mm.

The soft inclusion is heavily flattened when it enters the roll gap (Fig. 3b) at the same time as it is twisted clockwise similar to the hard one. Because of the shape of the plastic region at the entrance, the upper part of the inclusion enters the plastic region earlier than the part of the inclusion. Consequently the upper part is accelerated while the lower is still rigid and has the same low velocity as the incoming slab. This explains the clockwise rotation. Further more it is interesting to see that in (Fig. 1c) the inclusion has been twisted once again, this time however anti clockwise. Also this can be clarified, because the stream lines inside the plastic region become shorter towards the symmetry line. Consequently the inclusion bottom must increase its velocity from minimum at the entrance to maximum at the exit along a shorter stream line. This explains the higher velocity for the inclusion bottom and thereby the anti clockwise rotation. In (Figs. 1d-e) neither rotation nor flattening is observed.

Different indices are used for describing the behaviour of the inclusion and its surrounding matrix, which are found to be in total or partial contact. The

inclusion is described by is described by the well known index referred to Malkiewicz and Rudnik [28], Eq (1) and the formation of voids by Eqs. (8-9), page 36. The background of the equations becomes clear from Eqs. (2-7) together with (Fig. 4). The subscript  $m$  refers to the geometry of the hole, in which the inclusion is embedded and  $i$  to the inclusion itself.  $H_0$  and  $H_1$  is the slab thickness before and after a single pass reduction respectively.

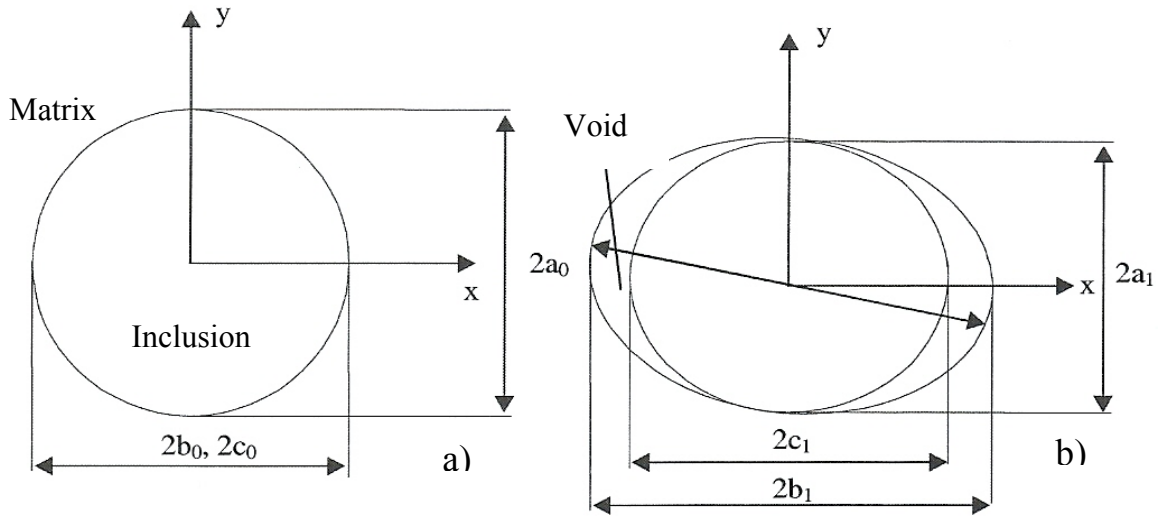


Fig. 4. Nomenclature used in Eqs. (1-9), (a) initial geometry, (b) geometry after one pass.

Results are presented in (Fig. 5). The curve based on the Malkiewicz and Rudnik index  $v$  shows, that for the soft inclusion, it increases from approximately 2 to 2.5 when the slab reduction decreases from 20% to 7%. For the hard inclusion the index equals zero. Thus the index shows that the soft inclusion is deformed more than the slab. This is true especially for light reductions. The “void index”  $(v_m - v_i) > 0$  illustrates that voids are formed around the rigid inclusion for all reductions studied. The maximum hole-diameter, in which the rigid inclusion is embedded, becomes big compared to the slab elongation especially for the light reduction in slab thickness.

Inclusions and the matrix around them are deformed dissimilarly at various distances from the slab surface (Fig. 6). Clearly the hard inclusion located close to the slab centre ( $3H_0/8$ ) is the most harmful one. Here two big voids are formed, one on each side of the inclusion, because of heavy tensile stresses close to the centre of the slab. An imagined line between them (marked red in Fig. 6) is found to be almost parallel to the line of symmetry. Closer to the surface however, this line gets more and more inclined (marked blue). Considering the soft inclusion (Fig. 7) no voids are found and its inclination to the axis of symmetry after a slab reduction of 13.6% is small and almost independent of its position.

$$\nu = \frac{\varepsilon_i}{\varepsilon_m} = \frac{1}{2} \frac{\ln \frac{c_1}{a_1}}{\ln \frac{H_0}{H_1}} \quad \text{Malkiewicz and Rudnik [28]} \quad (1)$$

$$\phi_i^x = \ln \frac{c_0}{c_1} \quad (2)$$

$$\phi_i^y = \phi_m^y = \ln \frac{a_0}{a_1} \quad (3)$$

$$\phi_m^x = \ln \frac{b_0}{b_1} \quad (4)$$

$$\phi_m = \sqrt{\left(\phi_m^x\right)^2 + \left(\phi_m^y\right)^2} \quad (5)$$

$$\phi_i = \sqrt{\left(\phi_i^x\right)^2 + \left(\phi_i^y\right)^2} \quad (6)$$

$$\phi_h = \ln \frac{H_0}{H_1} \quad (7)$$

$$\nu_m = \frac{\phi_m}{\phi_h} \quad \text{Refers to the hole where the inclusion is embedded} \quad (8)$$

$$\nu_i = \frac{\phi_i}{\phi_h} \quad \text{Refers to the inclusion} \quad (9)$$

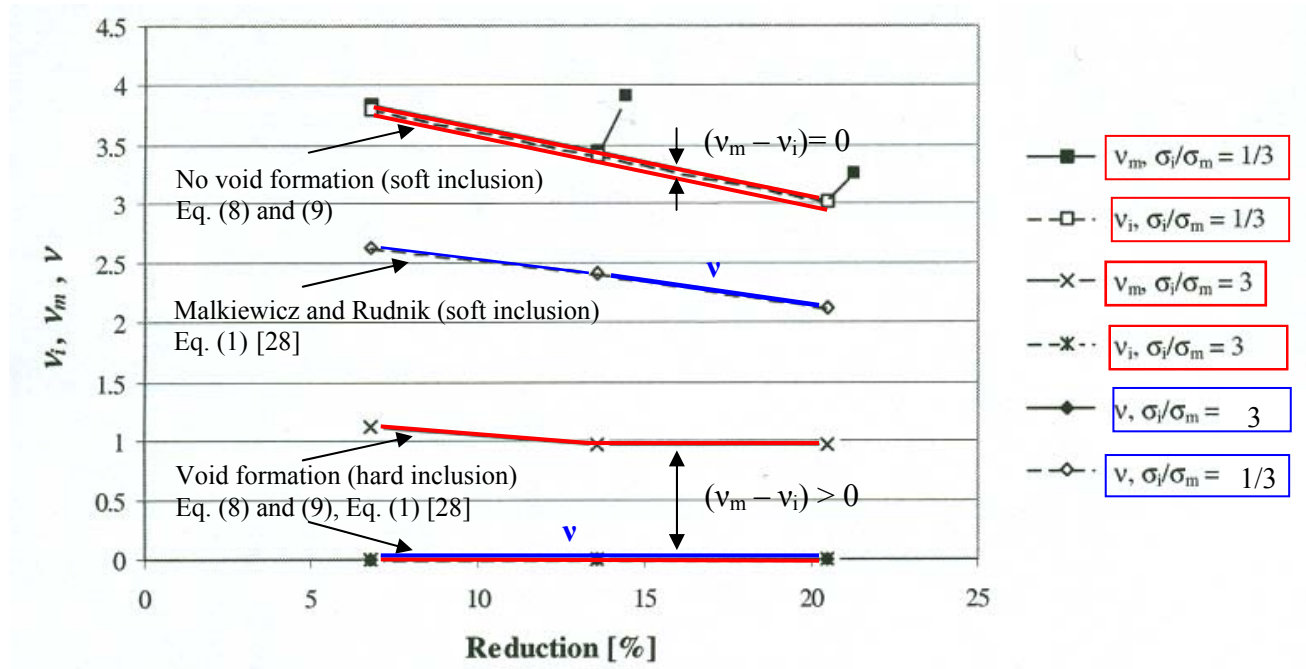


Fig. 5. Influence of single pass reductions on deformation indices for a hard and soft inclusion. The inclusion is positioned at a distance  $H_0/4$  from the slab surface. Initial slab thickness  $H_0 = 220$  mm and the initial inclusion radius  $c_0 = 4$  mm.

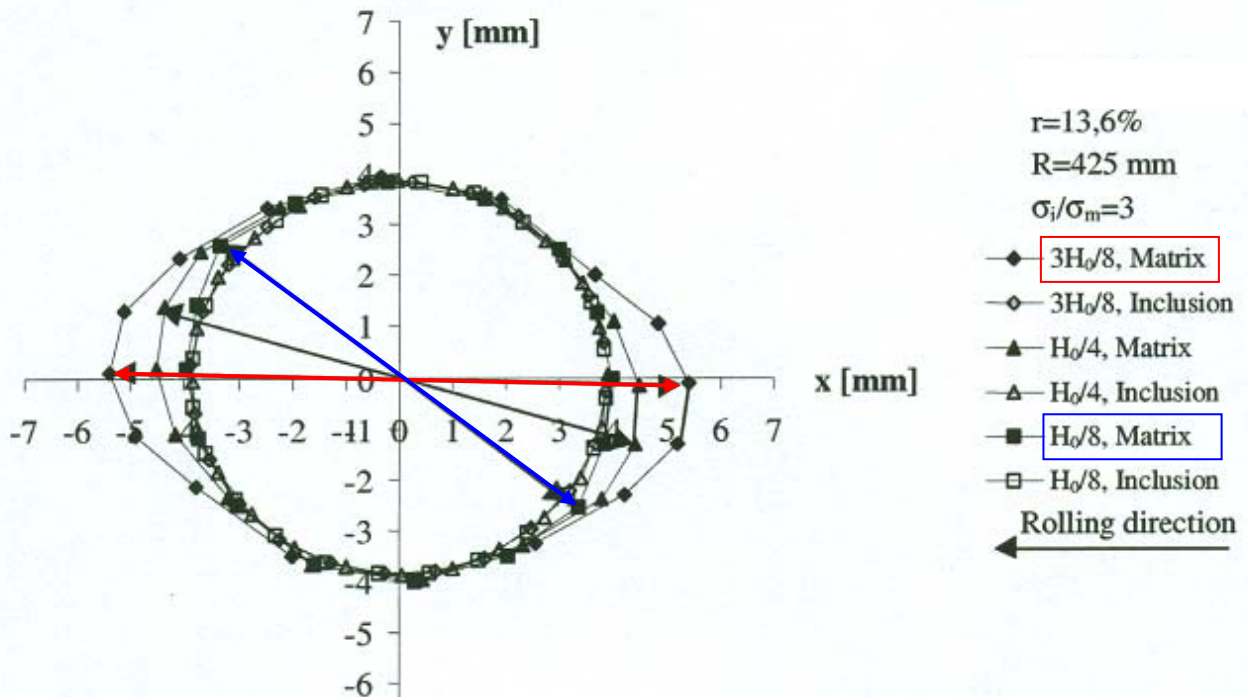


Fig. 6. Orientations of two opposite voids, found for hard inclusions at different distances from the slab surface. Initial slab thickness  $H_0 = 220$  mm,  $H_1 = 190$  mm and the initial inclusion radius  $c_0 = 4$  mm.

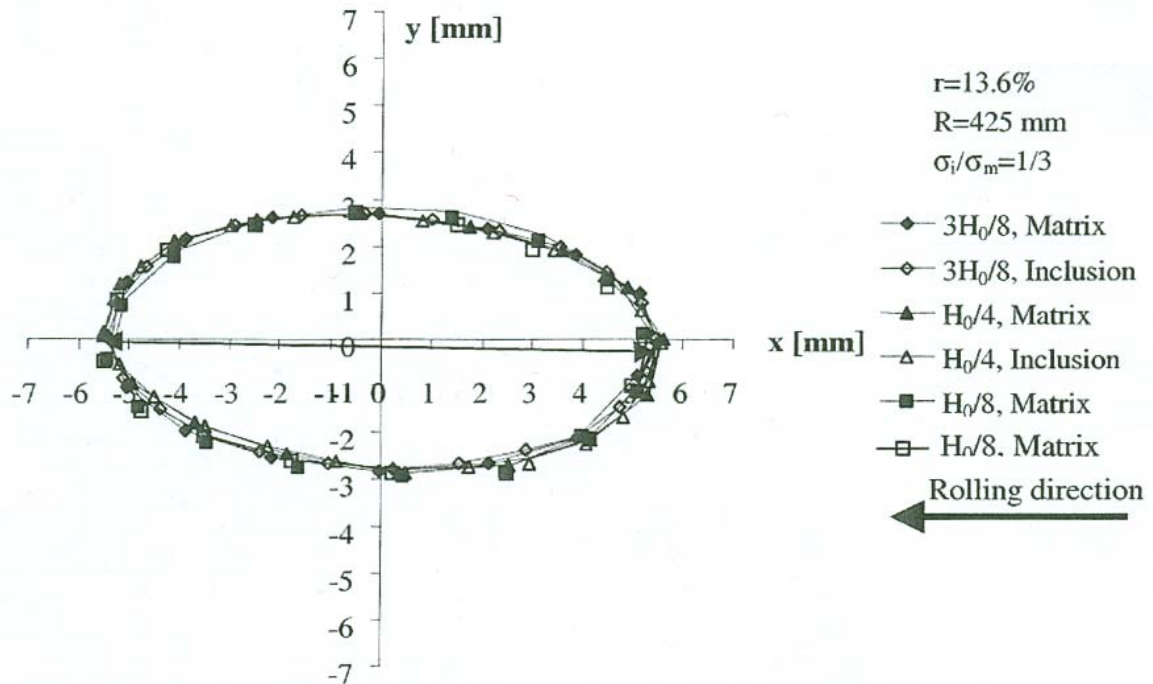


Fig. 7. The inclination towards the line of symmetry for soft inclusions located at different distances from the slab surface. No big difference is seen. Initial slab thickness  $H_0 = 220$  mm,  $H_1 = 190$  mm and the initial inclusion radius  $c_0 = 4$  mm.

According to the results presented in (Figs. 5) – obtained by means of the indices defined in Eq. (8) and (9) – together with the conclusions from (Fig. 6) the following recommendation for preventing void formation is extracted to industry: If hard macro inclusions are detected close to the centre of an as-cast slab a heavy reduction is proposed for the first pass because a heavy reduction means a higher hydrostatic pressure within the plastic region and thereby small voids compared to the reduction in slab thickness.

*Paper E* also treats the influence of roll radius and friction.

#### 4. Concluding remarks

The new die design proposed in forging, *Paper A*, reduced the number of blows from 9 to 6 and the aim of increasing the material yield by 1 kg was reached. The concept has been used in production during the years 1996-2003. The productivity was improved by 30-40%. Earlier 1000 crown wheels could be forged before the tool had to be taken out of production. The new design managed 1500.

The old pre-form shapes from the roller reducing mill are now exchanged from cross sections of rounds and squares to nothing but circular. For long components with a minor material flow in the length direction, the quasi-3D

method proposed *Paper B* is easy to use. It is considered valuable especially for small enterprises which cannot afford a research group of their own. What is needed is a 2D FE-code and access to experimental results for compensation of the material lost in the cross section, because of axial material flow.

The influence of rolling process parameters on the behaviour of longitudinal and transversal cracks is treated in *Paper C* and *Paper D* receptively. – It is concluded that longitudinal cracks can be totally closed. However this is done by folding the opposite side surfaces of the crack, with an oxide flake embedded in-between. This oxide deteriorates the product. In order to minimise its harmful effect on the product surface the following recommendations are given. Light drafts at the beginning of the rolling schedule followed by heavy ones. Doing so, the bottom part of the crack will be closed early and the embedded oxide film will be thin. And – during the finishing rolling, including heavy elongations of the workpiece, the thin oxide film will be broken up to pieces with a large area of virgin material ensuring a perfect bond. In this way it should be possible to improve the material yield. Only a thin surface layer should be necessary to remove by means of grinding. – Considering transversal cracks it is found that small drafts/pass mean that the crack width increases at the same time as the crack height decreases more rapidly than the slab thickness. Thus it is possible to eliminate them without any folding. The latter statement, however presupposes that reversal rolling is used. When such a crack has been eliminated the crack surface has been extended and coincides with that of the slab.

*Paper E* treats the behaviour of a hard and a soft inclusion in rolling. In the paper a void formation index is proposed and utilised. Considering the material yield, the influence of voids is of another character compared to the surface cracks. Large voids, found around big and hard inclusions in the slab centre may cause scrapping of the whole material. Big rolls and heavy reductions are recommended.

Finally it shall be pointed out that the ideas and the interpretations of results are to a large extent based on knowledge from classical methods of analysis such as the slab-, slip-line field- and upper bound method. The new concept proposed in the forging of crown wheels is based on the “friction hill” curve from the slab method. The rotation of voids and soft inclusions in rolling are explained by the shape of the plastic region as derived from the slip-line field method. The locations of the most critical voids were in good agreement with the low hydrostatic pressures derived by the same method. The author feels quite confident considering the FE-results because no qualitative disagreement is found between the methods.

## 5. References

1. B.-A. Behrens, E. Doege, S. Reinsch, K. Telkamp, H. Daehndel and A. Specker Precision forging processes for high-duty automotive components *Journal of Materials Processing Technology*, 185 (2007) 139-146.
2. G. Samolyk and Z. Pater, Application of the slip-line field method to the analysis of die cavity filling, *Journal of Materials Processing Technology*, 153-154, (2004) 729-735.
3. B. Tomov, R. Radev and V. Gagov, Influence of flash design upon process parameters of hot die forging, *Journal of Materials Processing Technology* 157-158 (2004) 620-623.
4. H. Keife and U. Ståhlberg The influence of flash design on material flow and tool pressure in closed die forging: a practical example, *Journal of Mechanical Working Technology* 9 (1984) 37-52.
5. M. Poursina, J. Parvizian and C.A.C. Antonio, Optimum pre-form dies in two-stage forging, *Journal of Materials Processing Technology*, 174 (2006) 325-333.
6. M. Sedighi and S. Tokmechi, A new approach to preform design in forging process of complex parts, *Journal of Materials Processing Technology*, available online 23 June 2007, In Press Corrected Proof.
7. J.J. Park and H.S. Hwang, Preform design for precision forging of an asymmetric rib-web type component, *Journal of Materials Processing Technology*, 187-188 (2007) 595-599).
8. U. Ståhlberg, Influence of spread and stress on the closure of a central longitudinal hole in the hot rolling of steel, *Journal of Mechanical Working Technology*, 13 (1986) 65-81.
9. C.Y. Park and D.Y. Yang, Modelling of void crushing for large-ingot hot forging, *J. Mater. Process. Technol.* 67 (1998) 195–200.
10. C.Y. Park and D.Y. Yang, A study of void crushing in large forgings, estimation of bonding efficiency by finite-element analysis, *Journal of Mechanical Working Technology*, 72 (1997) 32–41.
11. U. Ståhlberg, H. Keife, M. Lundberg and A. Melander, A study of void closure during plastic deformation, *Journal of Mechanical Working Technology*, 4 (1980) 51–63.
12. W. Johnson and P.B. Mellor, *Engineering Plasticity*, van Nostrand Co. Ltd., London (1973).
13. Z. Wusatowski , *Fundamentals of Rolling*, Pergamon Press, Wydawnictwo “Slask”, Katowice (1969).
14. C. Luo and U. Ståhlberg, A mesomechanical approach for studying the material behaviour close to non-metallic inclusions in steel hot-rolling, 2<sup>nd</sup> European Rolling Conference, Västerås, Sweden, May 24-26, 2000.
15. C. Luo and U. Ståhlberg, Deformation of inclusions during hot rolling of steels, *Journal of Materials Processing Technology*, 114 (2001) 87-97.
16. Hai-liang YU, Xiang-hua LIU, Chang-sheng LI and Y. Kusaba, Behavior of transversal cack on slab corner during V-H rolling process, *Journal of Iron and Steel Research, International*, 13 (2006) 31-37.
17. Form-2D, Finite element system for simulation and analysis of forming processes, User's Guide, Quantor Ltd., Moscow, 1995.
18. John O. Hallquist, *LS-DYNA Theoretical manual*, Livermore Software Technology Corporation, May 1998.
19. S. Kobayashi, S.-I. Oh and T. Altan, *Metal forming and the finite-element method*, New York and Oxford, Oxford university press 1989.

20. D. Flanagan and T. Belyotschko, A uniform strain hexahedron and quadrilateral and orthogonal hourglass control, *International Journal of Numerical Methods Engineering*, 17 (1981) 679-706.
21. L.E. Schwer, W. Cheva and O.J. Hallquist, A Simple Viscoelastic Model for Energy Absorbers Used in Vehicle-Barrier Impacts, *Computational Aspects of Contact Impact and Penetration*, Elmepress International, Lausanne Switzerland (1991) pp. 99-117.
22. C.A. Felippa, Interaktive Procedures for Improving Penalty Function Solutions of Algebraric Systems, *IJNME*, 12 (1978) 821-836.
23. E. Ervasti, Systematic methods for improving the material yield in hot forging, ISRN:KTH/MB-UND-0001-SE, ISSN:1104-7119, TRITA-MB-UND-0001, April 1955.
24. E. Ervasti and U. Ståhlberg, Improvements in the production of crown wheels by counter blow hammer forging, put forward at 16th International Forging Congress, IFC, in Beijing, China, September 9-16, 1999.
25. T. Altan, S-I.K. Oh, H.O. Gegel, *Metal Forming, Fundamentals and Applications*, American Society for Metals (1983), pp. 127.
26. S. Kalpakjian, *Manufacturing Processes for Engineering Materials*, Addison-Wesley, Reading, MA (1984), pp. 330.
27. C. Luo, Doctoral Thesis, Modeling the Behaviour of Inclusions in Plastic Deformation of Steels, Department of Production Engineering, Royal Institute of Technology, Stockholm May 2001.
28. T. Malkiewicz and S. Rudnik, Deformation of non-metallic inclusions during rolling of steel, *Journal of Iron and Steel Institute*, 201 (1963) 33-38.